Microwave augmented combustion synthesis of group VI nitride and carbide nanolayers on metal substrates:

Justin Bender, Tennessee Technological University, Cookeville, Tennessee
Juan A. Gonzalez, University of Puerto Rico, San Juan, Puerto Rico
2001 National Science Foundation
Research Experience for Undergraduates

The National Science Foundation
Professor Kenneth Brezinsky, Research Supervisor
Professor Christos Takoudis, REU Site Director
Department of Chemical Engineering
University of Illinois at Chicago
Chicago, IL

August 1, 2002

Table of Contents

Acknowledgements

Juan and I would like to thank the National Science Foundation for sponsoring the 2002 Research Experience for Undergraduates at the University of Illinois at Chicago.

Secondly, a special acknowledgement and thank you goes out to Professor Kenneth Brezinsky, our Research Supervisor for giving us the opportunity to work on such an enjoyable and relevant project. We hope the information amasses in this report is useful to you in future endeavors. We would also like to thank you for allowing us to make mistakes and really get a feel for the research process.

Appreciation is also given to Dr. Robert Tranter, for his help throughout my research work. A thank you to the following faculty, staff and students is also much deserved: Professor Christos G. Takoudis, REU Site Director; Professor Andreas Linninger for many helpful conversations and advice; Professor John R. Regalbuto; James Roman for machining the various apparatus and shop needs along the way; the staff in the office: Fred and Carol; and Professor Brezinsky's graduate students in the shock tube lab.

A number of individuals were extremely helpful in data analysis and we would like to thank them as well. Thanks to the staff at the Research Resource Center for their aid in performing microscopy: Dr. Allan Nicholls, Dr. John Roth and Dr. Kristina Jarousis. Professor Stephen Guggenheim's aid in x-ray diffraction analysis is greatly appreciated.

Figures

Tables

Abstract

Bulk transition metal nitrides and carbides have exhibited positive catalytic activity for commercially important reactions. When nitrides and carbides are present as nano-scaled over layers on these metal substrates the catalytic activity is enhanced further for hydrodenitrogentation and hydrodesulphurization reactions. The water-gas shift reaction, a critical step during the conversion of hydrocarbons into hydrogen gas rich feed for proton exchange membrane fuel cells, is also improved. More conventional methods of manufacture of nitrides and carbides, i.e reaction sintering, ion-beam assisted deposition and thermal cracking are slow and costly, yielding low conversion.

Microwave assisted combustion synthesis reactions in a vibrating fluidized bed, resulting in instantaneous reaction throughout, were performed for the synthesis of nitrides of group VI transition metals. This method has been investigated as means for controlling product morphology as well as initiating low adiabatic flame temperature reactions.

One to five micron sized chromium and molybdenum powders were fluidized in nitrogen gas and heated in the microwave to the point of reaction, followed by the pulsing of the microwave on and off to synthesize the group VI nitride over layers on its metal substrate. Heating of the metal powders is limited to a thin surface layer and fluidization aids in lowering the transport limitation of the nitrogen gas maximizing reaction potential yielding high conversion. Characterizations of the thin films were performed with SEM, TEM, EDS and XRD.

Amorphous 1-5 micron sized carbon black powders were thoroughly mixed with 1 -5 micron sized chromium and molybdenum powders. These mixtures were fluidized with argon and heated utilizing microwave energy to drive these low adiabatic flame temperature reactions. Characterizations of the products were performed with SEM, TEM and XRD. The application of these synthesizes for the water gas shift reaction to fuel cells will be addressed.

I. Introduction

The need for new types of materials has increased due to technical advances in industries such as electronics, petroleum, and aerospace. Advanced transition metal ceramics are compounds between at least one metallic element and one of the five non-metallic elements (boron, carbon, nitrogen, oxygen, sulfur). These advanced ceramic materials of transition metals due to their various characteristics (like high melting temperature, extreme hardness, electrical resistivity, magnetic susceptibility, superconductivity, and chemical resistance) have become important in the field of material science. These advanced ceramics have been shown to have applications in various industries. More specifically, past research has warranted a new push in the manufacture of Group VI transition metal nitrides and carbides.

Fuel cells are being developed to enable the commercialization of cleaner, more fuel-efficient vehicles. Many vehicle manufacturers favor proton exchange membrane (PEM) fuel cells operating with hydrogen from hydrocarbon fuels via steam reforming and/or partial oxidation. The water gas shift (WGS) is a critical step during fuel processing, and the associated reactor constitutes about one-half of the mass, volume, and cost of the fuel processor. While currently available catalysts work well in industrial petroleum refining and chemical plants, significantly improved catalysts are required to meet the transient operation and size constraints imposed by vehicular applications. Rather than seeking incremental improvements through the modification of existing formulations (e.g., Fe-Cr and Cu-Zn catalysts), researchers are developing new WGS catalysts based on transition metal carbides. Significant reductions in the WGS reactor size and cost are anticipated as a consequence of high activities, durabilities, and sulfur tolerance [1].

A. Overview of Combustion Synthesis

Combustion synthesis (CS) has attracted considerable interest in the last two decades due to its unique combination of technologically relevant characteristics. The method, in fact, makes possible the rapid synthesis of several highly refractory inorganic materials and advanced ceramics, thus avoiding the prolonged high temperature treatment, known as sintering, usually required in their conventional preparation. Refractory materials are resistant to thermal shock and are used to make crucibles,

incinerators, insulation, and furnaces, particularly metallurgical furnaces. Advanced ceramics are inorganic, nonmetallic, crystalline materials of rigorously controlled composition and manufactured with detailed regulation from highly refined raw materials giving the products precisely specified attributes desired by the producer**.** Reaction Sintering is the welding together of small particles of a ceramic material applying prolonged heat below the melting point resulting in improved mechanical and physical properties of the material.

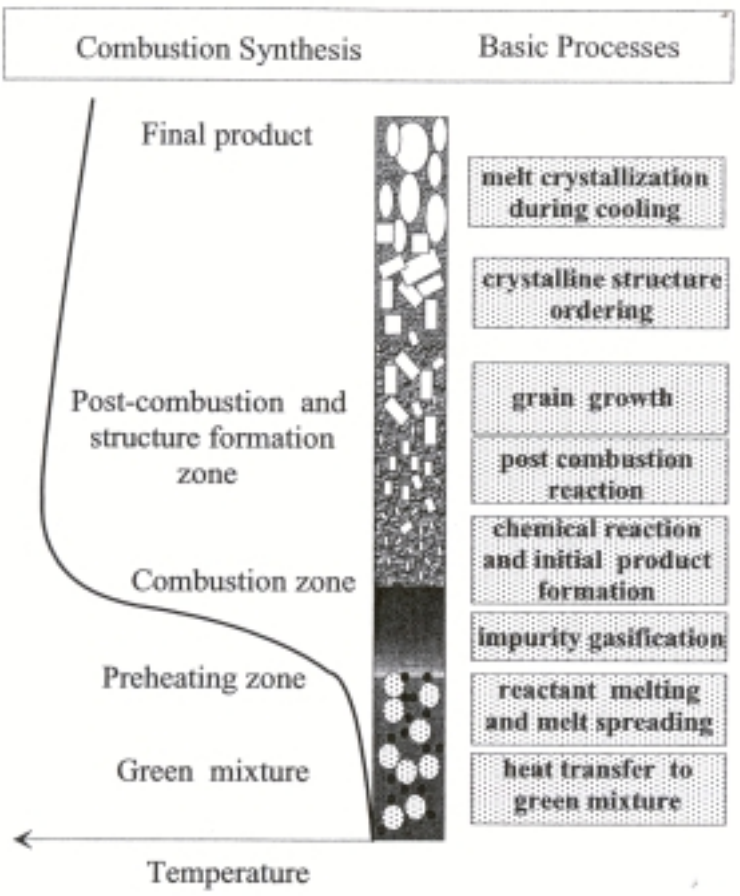

Figure 1: Schematic of Combustion Wave.

In this novel approach, the synthesis is obtained through an extremely rapid self-sustaining process driven by the large heat release by the internal energy of the reactants. The macroscopic characteristics of CS procedure resemble those observed in conventional combustion processes. The reactants, in form of fine powders, are usually dry-mixed. These mixtures are then placed in a controlled atmosphere and ignited through a resistively heated wire, a laser beam, or an electric discharge. Due to the enthalpy change between the reactants and products SHS reactions generally result in high combustion temperatures. The combustion synthesis reaction can be conducted in two modes [2]:

- Self-propagating mode (SHS)
- Simultaneous Combustion mode, or volume combustion synthesis (VCS)

The reactants are heated by an external source (e.g., tungsten or molybdenum coil, laser) either locally in SHS or uniformly in a furnace or microwave in VCS to initiate an exothermic reaction. It is interesting to note that many combustion synthesis reactions lie between these two types described. If the combination of thermo chemical and thermo physical properties of the system are appropriate, a high temperature reaction front (usually 1500-4000 °C) is initiated which then propagates through the mixture with a rate ranging from some millimeters to several centimeters per second for micron sized powders. The combustion wave propagates as shown in Figure 1 for mixtures consisting of two or more precursor powders. The initial mixture heats up and the contact between particles of starting mixtures is too limited for a chemical reaction to occur. Once the mixture's temperature rises to a certain point, impurities escape. Next, the reactant with the lower melting point coats other particles increasing the contact among the powders. At this stage, the chemical reaction is ignited. At the combustion zone, the leading edge of the heat wave promotes a full-blown reaction. Here, initial products are formed which may or may not be the same composition as the final products. Next, the final products begin to form from the heat released from the combustion wave followed by crystal growth and organization. Finally, the mixture cools into the final product [3].

A variant of this scheme involves one gaseous reactant. In this case, the reaction mixture is made of the powder(s) of the other non-gaseous reactant(s). This approach allows the synthesis of nitrides, hydrides, and oxides. Beside low energy requirements and the high reaction rate, the method has other advantages over the traditional methods, such as the simplicity of the experimental apparatus. Another demonstrated advantage is represented by the high purity of the products, which is largely due to the expulsion of volatile impurities under the extremely high temperatures in the wave. The reaction products are generally porous, but densification can easily be obtained through the application of a mechanical load just after the end of the reaction or simultaneous to it. Also, the high thermal gradients and rapid cooling rate can give rise to new non-equilibrium or metastable phases.

Combustion synthesis has been used to synthesize a large number of monolithic and composite inorganic materials (Table 1). These materials represent many varied functions and some of these materials in this table have been used or proposed for use in the following applications [4]:

- abrasives, cutting tools, polishing powders (e.g TiC, cemented carbides, and carbonitrides);

- elements for resistance heating furnaces (e.g. $MoSi_2$);

- high temperature lubricants (e.g. chalcogenides of Mo);

- neutron attenuators (e.g. refractory metal hydrides);

- shape-memory alloys (e.g.TiNi);

- high temperature structural alloys (e.g. Ni-Al intermetallic compounds);

- steel melting additive (e.g. nitrided ferroalloys);

- electrodes for electrolysis of corrosive media (e.g. TiN);

- coating for containment of liquid metals and corrosive metals (e.g. products of thermite reactions);

Table 1. Various inorganic compounds produced via Combustion Synthesis.

Compounds Produced via CS – [4]	
Borides	CrB, HfB_2, NbB_2, TaB_2, TiB_2, LaB_6, MoB_2, WB, ZrB_2, VB, VB_2
Carbides	TiC, ZrC, HfC, NbC, SiC, Cr_3C_2, SiC, B_4C, WC, TaC, VC, MO_2C
Carbonitrides	TiC-TiN, NbC-NbN, TaC-TaN
Cemented Carbides	TiC-Ni, TiC-Mo, WC-Co, Cr_3C_2 -(Ni,Mo)
Chalcogenides	MoS_2, $TaSe_2$, NbS_2, WSe_2, $MoSe_2$, MgS
Composites	TiC-TiB_2 , TiB_2 -Al_2O_3, B_4C-Al_2O_3, TiN-Al_2O_3, TiC-Al_2O_3 , $MoSi_2$ -A
Hydrides	TiH_2, ZrH_2, NbH_2
Intermetallics	NiAl, $NiAl_3$, FeAl, NbGe, TiNi, CoTi,CuAl
Nitrides	TiN, ZrN, BN, AlN, Si_3N_4 , TaN (cubic and exagonal)
Silicides	$MoSi_2$, $TaSi_2$, Ti_5Si_3, $ZrSi_2$, WSi_2, $NbSi_2$
Oxides	ZrO_2 , YSZ, $MgAl_2O_4$, $Bi_4V_4O_{11}$, $YBa_2Cu_3O_{7-x}$

- powders for further ceramic processing (e.g. Si_3N_4, AlN);

- thin films and coatings (e.g. silicides);

- functionally graded materials (FGM) (e.g.TiC+Ni);

- composite materials, cermets (e.g. TiC+Al_2O_3, Ni+YSZ);

- complex oxides with specific magnetic or electrical properties (e.g. $BaTiO_3$, $YBa_3Cu_3O_{7-x}$).

The general requirement for the application of this technique is the presence of a highly exothermic synthesis reaction, although a detailed analysis of all factors involved in the formation and

propagation of stable reaction fronts is quite complex. In the following section, a few of these considerations will be discussed.

1. Controlling Reaction Parameters

a. Characteristic Temperatures

During the combustion synthesis reaction there are four important temperature factors that may affect the process of the reaction and final product properties

- Initial temperature T_o which is the average temperature of the reactant sample before the reaction is ignited in the propagating mode
- Ignition temperature T_{ig} which represents the point at which the SHS reaction is dynamically activated without further external heat supply
- Adiabatic combustion temperature T_{ad}, which is the maximum combustion temperature achieved under adiabatic conditions
- The actual combustion temperature T_c, which is the maximum temperature achieved under normal configuration and non-adiabatic conditions.

The reactant mixture is generally ignited locally and the combustion front leaves behind the reaction products. In an idealized representation, the trend of macroscopic parameters representing the combustion process is reported in Figure 2(a). The reaction is limited to a very narrow region, 10-50 μm wide, in which the degree of conversion (η) goes rapidly from 0 to 1 while the

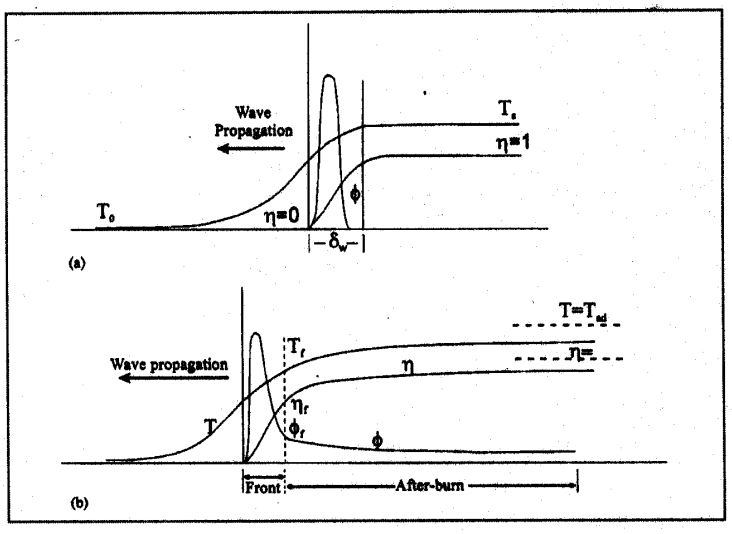

***Figure 2. Schematic representation of the temperature T, degree of Conversion η, and rate of heat generation ϕ, in an idealized combustion wave (a) and in presence of an after burn* [5].**

temperature increases to its maximum theoretical value, the adiabatic combustion temperature (T_{ad}). Heat is conducted ahead of the combustion front and the temperature corresponding to the onset of the chemical reaction is generally referred to as the ignition temperature (T_{ig}). The symbol ϕ in Figure 2(a) represents the rate of heat release, corresponding to the rate of the chemical process. In real processes, however, the reaction zone can be wider. This happens in the case of processes with a kinetic limitation. In this case the chemical reaction continues after the passage of the combustion front producing the so-called "after-burn phenomenon" (Figure 3b) [5].

Generally the presence of a largely exothermic reaction is considered an essential prerequisite for the feasibility of a combustion synthesis process. It is largely accepted that as an empirical rule of thumb, self-sustaining processes cannot take place unless T_{ad} >1800K. However, there are noteworthy exceptions. Several highly exothermic processes (with high T_{ad}) cannot produce self-sustaining combustion (e.g. the synthesis of TaC, Nb_5Si_3, and Al_2O_3 from the elements). Over the past two decades, investigations have demonstrated that CS reactions are complex processes, even more complex than gas-phase combustion, and their occurrence depends largely on the microscopic details of the reaction mechanism. Despite that, the adiabatic combustion temperature (T_{ad}) is still widely used in defining the feasibility of a CS process. It can be easily calculated for a given chemical process on the basis of its thermodynamic characteristics and the thermophysical properties of the products. Consider the reaction:

M(s) + X(s) = MX(s) (1)

Where a solid metal M and a solid non-metal X react to form a solid product MX.

The T_{ad} is the maximum temperature to which the product can be raised if the exothermic reaction is performed in adiabatic conditions. Its value can be calculated on the basis of the following general equation [6]:

$$\Delta H_{f,298} = \int_{298}^{T_{ad}} C_p \, dT \qquad (2)$$

where $\Delta H_{f,298}$ is the enthalpy of formation of MX(s) at T_o and C_p(MX) is the molar heat capacity of the solid product. It has been demonstrated that T_{ad} exhibits a roughly linear functionality with the ratio $\Delta H_{To}^{o}/ C_{p298}$ i.e. the ratio of the heat of formation and the heat capacity of the product at 298K. The observed linearity is a consequence of the relatively low sensitivity of the C_p function to temperature for certain compounds. It

has been empirically concluded that reactions will not be self-sustaing unless T_{ad}>=1800K which corresponds to $\Delta H_{To}^{o}/ C_{p298}$ >=2000K [2]. Equation (1) is valid only when the products are all solids and do not undergo phase transitions. In the case of phase transitions and partial or total melting of products Equation (2) is modified as follows:

$$\Delta H_{f,298} = \int_{298}^{T_{ad}} C_p(\alpha)dT + \Delta H_t + \int_{t}^{T_m} C_p(\beta)dT + \nu\Delta H_m + \int_{T_m}^{T_{ad}} C_p(liq)dT \quad (3)$$

where α and β are two different phases of the solid product, T_m is the melting point of the β phase, ΔH_t is the heat of transition between the α and the β phase, ΔH_m is the heat of fusion of the β phase, ν the fraction of solid β that is melted, and C_p (liq) is the heat capacity of the liquid product. The temperature of the combustion front is generally lower than the adiabatic temperature due to heat loss. Another important factor is that at such high temperatures the final products may not be stable and would decompose to give the original reactants. This lowers the conversion yield of the final product and also the adiabatic temperature calculations for the system. In this work the adiabatic temperatures of the discussed reactions have been calculated using a thermodynamic software package Chemsage, which takes into account all these factors.

The adiabatic temperature is an important factor in determining the self-sustainability of the reaction, but due to heat losses to the environment and heat transfer to the adjacent reaction mixture, which is still below the ignition temperature, reaction conditions are seldom adiabatic. Thus heat losses can result in a change in the reaction front velocity, stability and the actual combustion temperature T_c. Decreasing the heat generation and increasing the heat dissipation can create instabilities and may result in slowing down or temporarily halting the propagation of the combustion wave, or can even quench out the reaction. The combustion wave front propagates in a steady-state or non steady-state mode. A non steady-state mode is defined as a "non-uniform velocity of the combustion wave with respect to time and/or space" [7]. The non-steady-state mode is generally manifested in three forms [7]:

- Oscillation
- Spinning or spiraling
- Repeated combustion wave front movements

Instability of the combustion wave can lead to the extinction of the combustion wave. According to Munir et. al. 1998 "oscillatory motion of the combustion front results in a layered structure of the products, while the spiral motion may be predominantly associated with a surface reaction and hence bulk of the sample can remain largely unreacted after passage of the reaction front". The repeated combustion form of unsteady propagation is related to the kinetics of the reactions, especially in solid-gas reactions. The first combustion wave is relatively fast and localized along the exterior surface, while the second wave is slower and the combustion zone is much broader. The limiting parameter in this case is the diffusion of the reactants into the interior of the reactant mixture.

b. Ignition Techniques and Conditions

In contrast with the adiabatic temperature the ignition temperature cannot be easily calculated. It represents a very complex quantity strictly related not only to the thermodynamics and the thermophysics of the system, but also to the details of the reaction mechanism. As a general rule, ignition of a CS process is obtained when a small but significant layer of reactant powder is heated rapidly above the temperature where the rate of the chemical reaction is high enough to obtain a heat release higher than the rate of heat dissipation.

c. Degree of Dilution

The value of T_{ad} of a process can be modified to some extent. If the temperature of the reactants is raised above room temperature before ignition the combustion temperature will be also increased [Equations (2) and (3)]. In other words, sample preheating can be used to increase the combustion temperature. This practice is fairly common in the case of low exothermic reactions, when is difficult to obtain self-propagating reactions. On the other side, the combustion temperature can be reduced through the addition of inert phases to the reacting mixture. This procedure reduces the overall release of heat per unit volume of the mixture and “soaks” up some of the generated heat. The products of the same reaction are generally used as diluents, in order to avoid polyphasic products and control the combustion wave to some extent.

d. Green Mixture Density

The degree of compaction of the reaction mixtures strongly influences the reaction characteristics and the product microstructure. Green Density, also known as pressed density, is the weight per unit volume of a reacted compact. An increase in green density produces better contact between the grains of the reacting powders, but also increases thermal conductivity. The two phenomena produce opposite effects on CS processes. The increase in grain contact enhances the overall reaction rate and the degree of its completion, but a higher thermal conductivity increases heat conduction away from the reaction front reducing the possibility for the process to remain self-sustaining. This last effect is particularly relevant for metallic reactants, where very high values of thermal conductivity are obtained for dense samples.

The sample porosity plays an obvious crucial role in the case of solid-gas combustion processes, as in the case of the synthesis of nitrides and oxides. In this case only the external surface of the sample has direct access to the gas while the conversion of the sample core requires permeation of the gaseous reactant through the pores. In this case a surface combustion is generally observed followed by a long after burn. As a result, a very high degree of porosity is required in order to attain full conversion of the solid reactant. However, when the T_{ad} of the reaction is higher than the melting point of the reacting metal, the use of a highly porous sample results generally in a poorly converted sample. This behavior can be explained on the basis of the higher extent of melting of the reacting metal due to the higher degree of heat release in low-density samples. The melting of the metal causes a reduction in the porosity resulting in a largely unconverted sample core. This behavior is well represented in the case of the synthesis of TiN where a maximum is observed in the dependence of the degree of conversion of the sample on relative density. Changes in the sample green density affect also to some extent the microstructure of the final products. Examples have been found in the synthesis of some intermetallic phases, particularly aluminides, where the spreading of the low-melting reactant through the pores plays a major role in defining the characteristics of the final products. An intermetallic compound is any of a class of substances composed of definite proportions of two or more elemental metals, rather than continuously variable proportions (as in solid solutions).

e. Particle Size

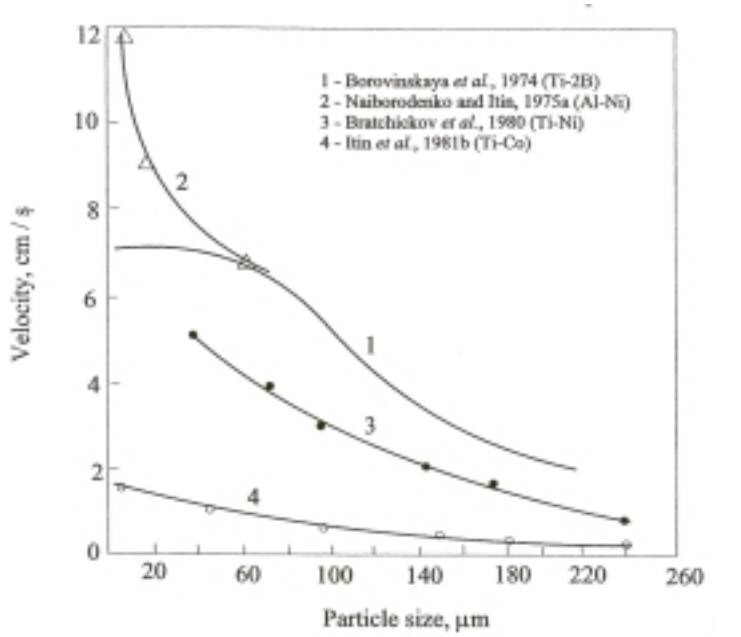

***Figure 3. Effect of metal (Ti ,Al) particle size on combustion velocity in systems with both melting reactants* [2].**

Along with sample porosity, particle size plays a major role in defining the characteristics of the reacting mixtures and of the reaction conditions. Since the stability of the combustion front depends largely on the rapid kinetics of heat generation, it must be expected that CS processes are generally favored in smaller particle size reactants. However, the details of the dependence of the reaction characteristics on the reactants particle size are quite complex and have been studied in depth only for a few processes, such as the synthesis of TiC and of a few intermetallic compounds. Generally, it is confirmed that an increase in particle size results in a marked decrease in the propagation rate of the reaction front. However, it should be kept in mind that in most combustion synthesis processes one or more of the reactants, generally the metals, melt. In such a case no dependence on the particle size of that reactant is generally observed.

f. Other Effects of Combustion Conditions

In addition to the reaction parameters already considered, there are further conditions that affect the CS process. These parameters range from the initiation of the SHS process (i.e. using different temperatures to ignite the combustion wave), initial temperature of the reactants (i.e. generally, higher initial temperature, yields a faster combustion wave velocity), and the effects of gravity on the system. The stoichiometry of the reactant powder mixture is another important process parameter, which significantly affects the SHS reaction and product properties. Any deviation from the stoichiometric ratio required to produce a certain product results in a decrease of the adiabatic temperature. The addition of excess product as a diluent is mostly used to control the reaction process.

B. Microwave Assisted Combustion Synthesis

Two important aspects of microwave assisted combustion synthesis are its instantaneous and volumetric heating characteristics. Therefore, the entire mixture reacts uniformly throughout, at the moment of heating.

Microwave heating has other advantages as well. The heating is outward from the center, giving rise to inverse temperature gradients. This can lead to different microstructures. Also, since the heating is instant, microwave power can be used to control the extent of reaction. The potential of microwave heating to control the extent of the reaction and possibly yield nano-overlayers of ceramic on metal substrates can be explained as follows. Microwave energy can interact with metal powders as well as non-metals. The power absorbed per unit volume (W/m^3) provides the following basis for heating [8,9].

$$P = \sigma |E|^2 \tag{4}$$

where: σ = total effective conductivity = $2\pi f \varepsilon_o \varepsilon_r \tan\delta$
E = local electric field
f = frequency of microwave
ε_o = permittivity of free space
ε_r =relative dielectric constant
$\tan\delta$ = loss tangent = $\varepsilon''/\varepsilon'$
where: materials complex permittivity = $\varepsilon^* = \varepsilon' - i\varepsilon''$

$$E = E_o \exp(-\frac{x}{d}) \tag{5}$$

where: d = skin depth or depth to which microwaves penetrate
E_o = maximum electric field generated

The skin depth is a strong function of frequency of the field

$$d = \frac{.0675}{f(Ghz)\sqrt{\varepsilon' \sqrt{1+\tan\delta} - 1}} \tag{6}$$

Since the effective conductivity σ for metallic samples is 10^6 to 10^{16} higher than for non-metal dielectric materials, at 2.45 GHz the skin depth for metallic samples is sometimes a few micrometers or less. Hence the absorption of microwave energy is by a relatively thin outer layer, which then transmits energy by conduction to inner layers [9]. According to Cherradi et al. 1994, “the heating of metals is attributed to eddy current losses from the magnetic fields.”

The demonstrated heating of metal particles by microwaves leads to the following hypothesis: since the heating of the metals is limited to a thin surface layer the probability of reaction with a non-metal at this surface layer is a maximum and would lead to a ceramic over layer formation. Furthermore, since microwave heating is instantaneous, switching the microwave on or off can control the reaction. Thus switching the microwave on would lead to reaction and if the reaction has not reached the self-sustaining stage, switching the microwave off would stop the reaction. For reactions that would not be self-sustaining because of a very low adiabatic flame temperature, microwave energy may also be used to drive these reactions at stoichiometric conditions. For reactions having a low flame temperature because of extremely low concentration of one reactant, microwave heating may also be used to promote reaction.

C. Combustion Synthesis in a Fluidized Bed

More traditionally, fluidized beds have been used to decrease the transport limitation of a gaseous reactant in many combustion processes. In Combustion Synthesis of bulk nitrides and carbides, one of the limitations in producing phase pure products is this very aspect.

Fluidized beds are characterized by a bed of solid particles acted upon by a fluid stream with sufficient velocity to suspend the solid particulate matter and force the gas through the bed. A point fluidization is reached when the upward drag force exerted by the fluid on the particles is equal to the apparent weight of the particles in the bed. Three main classifications of fluidized beds are: fixed, bubbling and circulating fluidized beds. The type of fluidizing bed used in these experiments is the circulating fluidized bed, which is characterized by the levitation of the majority of the solid bed material by the fluidizing gas. Increasing the fluidization gas velocity above the velocity of the solid particles does this. Also, it is seen that the pressure drop is nearly equal to the force exerted by the particles per unit area indicating that the powders are fully suspended.

$$\text{Pressure drop} = h\rho g \ N/m^2 \qquad (7)$$

This is important in the production of over layers because the particle is suspended in the gas stream thereby maximizing the effects of microwave heating and increasing nitrogen transport to the outer surface of the particle. It ignites the exothermic reaction and sparking with varied colors, collimated streaks of light and in some cases flame.

D. Group VI Transition Metal Nitrides and Carbides

1. Previous Work on Transition Metal Nitrides and Carbides

Transition metal nitrides and carbides, especially with nano-scale features have been shown to be potential replacements for traditional hydrodenitrogenation (HDN) and hydrodesulphurization (HDS) catalysts [11-13]. Removing the heteroatoms, i.e. nitrogen and sulfur, from energy producing hydrocarbons leads to cleaner and efficient burning and processing. The ability of catalysts to remove these heteroatoms is enhanced when the transition metal carbide or nitride is present as a nanoscale surface over layer on a metal substrate [11]. Nanocrystallites of molybdenum nitride and carbide have been shown to have catalytic activity for HDN and HDS equal to or greater than that of commercial sulfided molybdenum catalysts [13-16]. Commercially available ultra fine platinum powder has also been used to demonstrate that a porous aggregate of nanoscaled molybdenum carbide particles produced by sonochemical methods has enhanced catalytic activity for dehydrogenation of cyclohexane [17]. These studies thus show that enhancement of catalytic activity is associated with nano-scaled features of the transition metal nitrides and carbides. Also in hydrodesulfurization of petroleum, carbides are found to offer improved hydrogen economies. They are more resistant to poisoning by sulfur [18].

Carbides have also been demonstrated to be highly active water gas shift reaction catalysts, even more superior to the commercially used Cu-Zn-Al catalyst [19]. With optimization of their compositions and microstructures these materials could reduce the reactor size of the Water Gas Shift reactor. WGS is a critical step during the conversion of hydrocarbons and alcohols into H2 rich feed for proton exchange membrane (PEM) fuel cells. These fuel cells are leading candidates for use in vehicles, portable electronics and residential power sources.

Also carbides can be used as electrodes in ultra capacitors. These are high power energy storage devices that can be used to load level batteries and fuel cells in portable electronic devices like cellular phones and hybrid vehicles. Advanced ceramics are also used extensively in electroceramics, the basic material for microchips, insulators, fiber optics and capacitors. The carbides of major interest are those of group IV, V and VI transition metals; particularly group VI for their catalytic activity.

The method generally used to from these nitrides and carbides is by use of metal, metal oxide or metal hydride powder that is reacted with carbon or nitrogen at elevated temperatures for relatively long

processing times [11-12]. In these temperature programmed reaction methods, exposure to heat for long processing times may result in grain growth and thus change in the morphology of the product. Thin nano-scale over layers is generally formed by thermal cracking of a hydrocarbon on the metal or by thermal reaction of ammonia or nitrogen at the metal substrate surface [12]. Another method to form nanocrystallites is by use of sonochemical methods [17]. Also, ion-beam assisted deposition is used to form thin over layers of ceramics [12]. These methods are slow and in most cases the yield is low. Whereas the self-propagating high temperature synthesis (SHS) technique used in this work allows many advantages including, short reaction times, better product purity, and better control over product morphology. These benefits combined with microwave heating in a fluidized bed leads, at least in theory, to yield over layers of ceramics on a powder metal substrate.

2. Scope of the Present Work

Transition metal nitrides and carbides were demonstrated in work surface scale tests to be highly active for the WGS reaction. Present work focused on further improving the synthesis of the nitrides and carbides to prepare the catalysts in the appropriate form for testing in a water-gas shift reaction. Several promising formulations have been identified. The normalized surface area reaction rates for some of the materials are substantially higher than those for commercial catalysts. Both the nitride and carbide samples were also stable in the presence of steam and air to temperatures of 600°C and 300°C, respectively; however, their surface areas will have to be increased to yield viable alternatives to the commercial WGS catalysts. As part of the effort, the manufacture and characterization of Group VI transition metal nitrides and carbide nano over layers on their metal substrates was performed. The information accumulated here, will guide the design of the next generation of water-gas shift reaction catalysts for use in proton exchange membrane fuel cells.

II. The Experiment

A. General Experimental Apparatus and Set-up

The demonstrated heating of metal particles by microwaves leads to the following hypothesis: since the heating of the metals is limited to a thin surface layer the probability of reaction with a non-metal at this surface layer is a maximum and would lead to a ceramic over layer formation. Furthermore, since microwave heating is instantaneous, switching the microwave on or off can control the reaction. Thus switching the microwave on would lead to reaction and if the reaction has not reached the self-sustaining stage, switching the microwave off would stop the reaction. For reactions that would not be self-sustaining because of a very low adiabatic flame temperature, microwave energy may also be used to drive these reactions at stoichiometric conditions by sustaining the reaction.

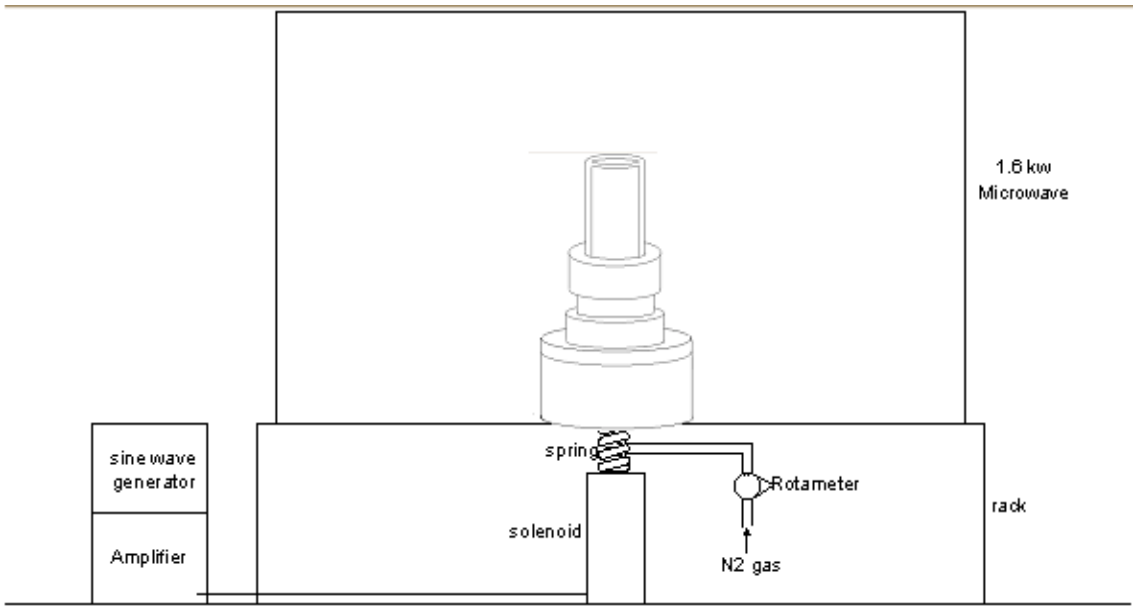

Figure 4: Schematic of experimental setup where the microwave is used as ignition source.

The schematic of the experimental setup for using the microwave as a heating source is shown in Figure 4 and a photograph for the setup in Figure 5. A hole has been drilled through the bottom of the microwave to allow for the fluidizing gas tube. The microwave used is a domestic microwave Amana Radar Range (1.6 kW) oven with a microwave frequency of 2.45 GHz. Reactions were carried out in both 13.5 mm i.d. and 19 mm o.d. and 25 mm i.d. and 30 mm o.d. quartz tubes purchased from Quartz Scientific

Company (Fairport Harbor, Michigan) in lengths of 121.92 cm (48 inches). These 4 ft. tubes were cut with a diamond tipped saw into 6 in. sections. The majority of the experiments performed were carried out in a 25 mm i.d. and 30 mm o.d. quartz tube to reduce heat loss from the powder bed and aid in fluidization.

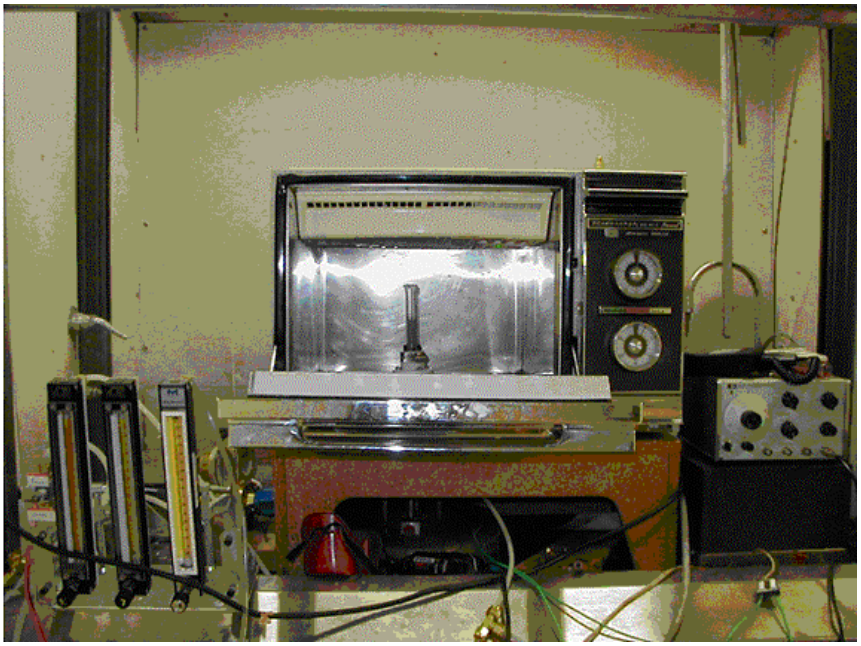

Figure 5: Photograph of experimental setup where the microwave is used as ignition source.

There were evident flaws in the experimental set-up left from previous work. First, one of the problems involved the materials used in the machining of the reaction base that facilitates the transfer of fluidizing gas to the quartz tube. These bases were manufactured to withstand short reaction times in a microwave, not extended reactions. Teflon is an adequate material to use in extended microwave heating; however the fact the apparatus was in two connecting pieces was the issue. Macor (a glass ceramic) is not a compound capable of withstanding extended heat treatments in a microwave environment. Extended heating resulted in the thermal breakdown of these materials due to hot fluidizing gas destroying the integrity of the connection with in the interior of the base. This problem was rectified through the machining of a one-piece stainless steel base with similar dimensions. Screw threads were cut 1” into the top of the interior of the base.

Secondly, trying to accurately reproduce the fluidization technique using the method of Akhil Jain proved to be a struggle. The gas velocity required to produce the desired circulating fluidized bed would always result in the expulsion of the quartz tube from the connector piece held in place within the Teflon base by a VITON O-ring. Through the design and machining of a replacement fixture, this problem was averted for subsequent reactions. The hold of the tube is achieved with a three-piece stainless steel holder: a female and male steel column and compression ring (Figure 6). A -123 standard VITON brand O-ring (purchased from McMaster and Carr, Chicago, Illinois) is placed in the angled slot between the male column and the quartz tube. The compression ring rests snugly on top of the O-ring and the overlaying female column places pressure on the ring creating a seal with the quartz tube capable of withstanding substantial gas flow during reaction. A portion of the tube holder was cut away at the base leaving an area where threads were cut into the surface. On the underside of the tube where the portion was cut away, a groove was placed where a -227 VITON O-ring rests snugly against the underside of the tube holder and the top of the base.

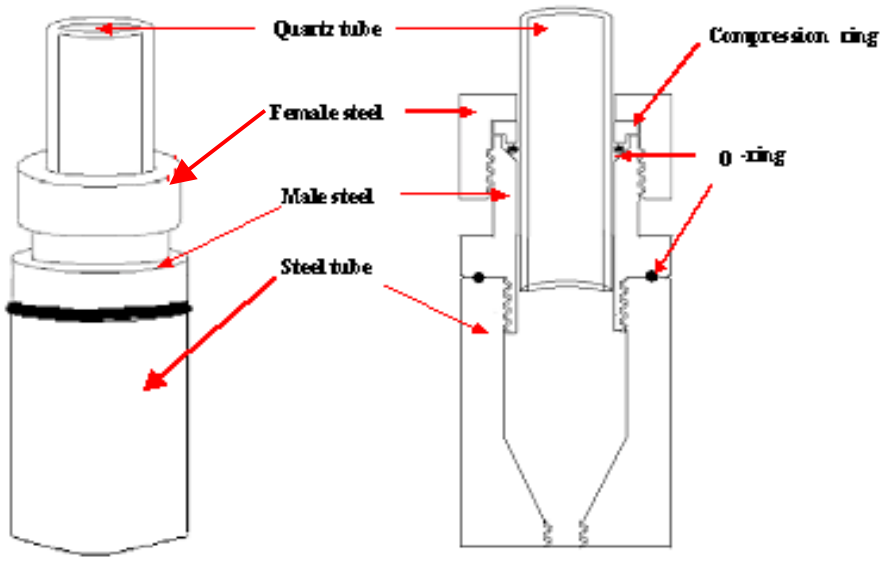

Figure 6: Schematic of improved quartz tube holder and steel base experimental apparatus.

The basic procedure for carrying out the reactions is as follows. The metal powder (and non-metal powder in case of carbides) is dried in the oven at 60^{o}C for two hours. For the case of the carbides, the

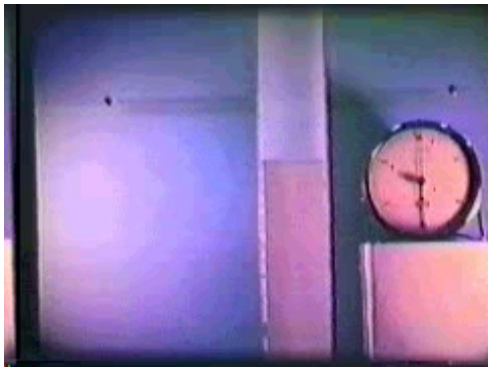

Figure 7: Initial particle bed position in an expanding fluidized bed set-up.

Figure 8: Final particle bed position in an expanding fluidized bed set-up.

reaction mixture is calculated to yield the desired stoichiometric ratio and dry mixed for four hours with millstones of varying size in a Nalgene bottle. The quartz tube is filled with the powdered reaction mixture (in case of reaction between a metal and a solid non-metal or only with the metal powder in case of solid gas reaction) and sealed from both ends with a stainless steel sieve. A variation in the procedure was used in comparison to the method of Akhil Jain. Akhil filled each reaction vessel half full of reactants. The fluidized bed employed with this method involved an expanding bed. With a large amount of precursor mixture filling the quartz tube, a gas flow rate capable of expanding the particle bed to fill the quartz tube is easily reached. Figures 7 and 8 show an expanding fluidized bed. Figures 9 and 10 exhibit the particle-to-particle interaction view of this method. The gas flow is constant throughout the particle bed, particle to gas interaction is consistent during reaction and the gas transport limitation problem is solved

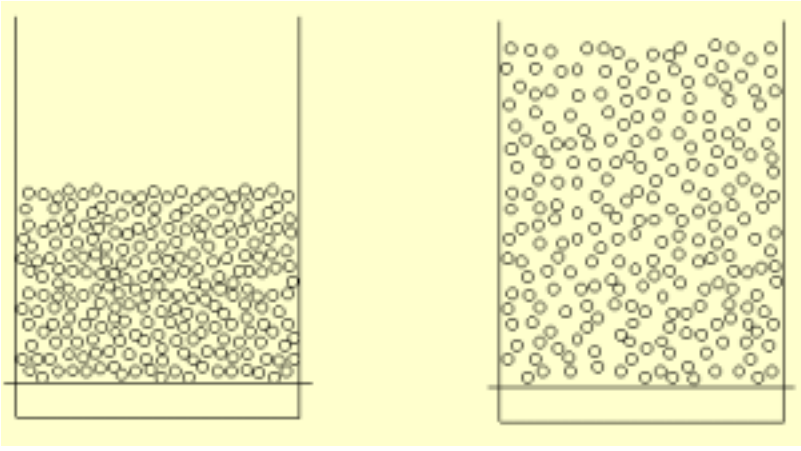

Figure 9: Schematic of initial particle bed position in an expanding fluidized bed set-up.

Figure 10: Schematic of final particle bed position in an expanding fluidized bed set-up.

A variation of this method was performed for the current work due to the large mass of metal particles required to achieve this fluidization. A circulating bed was used to minimize the amount of precursor powders needed for each experiment (Figure 11). The transport limitation was still solved. However inherent with this method, particles were lifted from the particle bed where reaction with the fluidizing gas was uniform around the surface of the particle and recycled as the bed churned over on itself. This method was employed to maximize the number of experiments that could be performed. It is apparent to the author that the method employed by Akhil Jain would result in better product attributes including uniformity in over layer formation and an increase in percentage of particles that react in terms of producing nitride over layers. However, for the case of the carbides, where both of the reactants were solid particles, it was important to maximize the collision frequency. This will be explained further in the carbide section of the experimental portion of this paper.

Figure 11: Overview of circulating fluidized bed as utilized in the current work.

The seal of the sieve is very important in the outcome of the experiment. A circle is cut corresponding to the size of the o.d. of the quartz tube (30 mm or 19 mm). The ceramic is placed as a thin presence along the outer wall surface at the top of the tube. It is important to have enough to successfully hold the sieve in place, but no more. The sieve is placed by pressure applied on the middle of the outside of the screen with a blunt object. Careful mixing of the ceramic must take place in order to have a consistency that is not to thin as to fuse the sieve closed in areas where hardener was not desired. This preliminarily sealed tube is baked in an oven at 250^{o}C for 30 minutes. Once this ceramic has successfully set, more ceramic is added around the existing seal, as needed, to fully seal the tube and once again baked for a total

time of 2 hours. Two mesh sizes of the stainless steel sieves are used. One is 645x1400 and the other is 325x2300. The difference between the two is in the nominal particle size retention. The 325x2300 mesh sieve has 2-micron nominal particle retention whereas the 645x1400 has approximately 5-micron nominal particle retention. In nitride experiments, fluidization is easily obtained with –325 mesh particles using the 645x1400 steel sieve. The carbide experiments, where the nominal size of the carbon is very important, i.e. 1-5 microns, require the 325x2300 steel sieve is used.

Once, a solid seal is obtained in one of the ends of the tube, the reaction mixture or precursor powders are placed in the tube corresponding to a mass of 5 to 10 grams. The assembly process is as follow. With the sealed end of the quartz tube flat on a table, the female steel column is placed. Next, the compression ring is fit over the end of the tube and a -123 VITON O-ring is placed over the compression ring. The male steel column is screwed on to tighten the O-ring around the outside of the tube. Enough room must be left protruding from the end of the male steel column as to allow application of the remaining sieve. Once the tube is locked into place, the sieve is attached as described above. Finally, the tube holder is screwed into the steel base and sealed with the -223 VITON O-ring.

The apparatus is assembled as described above and screwed into the bottom of the microwave where fluidizing gas (nitrogen in case of nitrides, and argon in case of carbides) is passed through the rotameter to obtain stable fluidization. The fluidized bed setup is vibrated with the help of a solenoid when particles around 2 to 5 microns are used, which are cohesive and fall in the Geldart group C category. The vibration reduces the agglomeration and produces a much more stable bed, whose height is less than that of the bed obtained without vibration. The pressure drop can be measured approximately by using a U-tube manometer with one open end and the other end attached to the fluidizing gas tube inlet. Also, it is seen that the pressure drop is nearly equal to the force exerted by the particles per unit area indicating that the powders are fully suspended.

B. Characterization Techniques and Equipment

1. Scanning Electron Microscopy with Energy Dispersive Spectrometry

Scanning electron microscopy (SEM) was performed on all precursors samples and various product samples to examine their morphological characteristics. The instruments used for this

characterization was a Hitachi S3000N variable pressure. Also Energy Dispersive X-ray spectrometry (EDS) was performed on all samples with the X-ray detectors. Use of low energies limits the penetration of the electron beam, thus giving elemental information of the surface. Also morphological characteristics of the surface are highlighted more if the SEM is used at a low kv. This technique is very useful in characterizing surface layers of the product for nitrides. In the case of the carbides, however, the free unreacted carbon interacts with EDS and can yield false results.

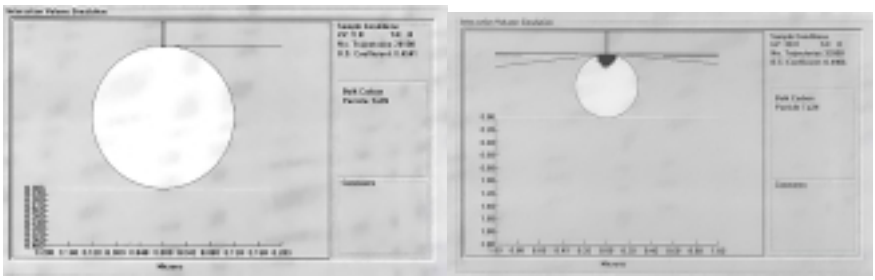

Figure 12(a) and (b): Simulation of electron beam for S3000N Variable pressure SEM showing electron penetration at 5kv and 30kv for Ta2N particle.

2. Transmission Electron Microscopy

The samples were also analyzed by transmission electron microscopy to visualize the reaction zone, verify the presence of the over layer, quantify the depth of reaction and view the resulting *d* spacing. The instrument used is JEOL 3010. The samples were crushed in a mortar and pestle and mixed with ethanol to slurry. This slurry is applied to a holey carbon grid using a micropipette with enough particle distribution as to observe an even dispersion of particles under 10x light microscope magnification. High-resolution images are obtained showing the interplanar atomic spacing and these are compared with the literature interplanar atomic spacing corresponding to the Joint Committee of Powder Diffraction Standards or JCPDS data to determine presence of different phases. Using Digital Micrograph, imaging software used in conjunction with the JEOL 3010, the atomic *d* spacing is accurately measured.

3. X-ray Diffraction

A Siemens D5000 powder diffractometer is used for the study. The sample is placed in powder form in a backfill sample holder. The machine scans through an array of angles as set in a range from 20-90^{o} and collects data on the scattering of the x-rays via a Geiger counter. Software (MDI Jade 5.1) housing

all current JCPDS data is used to analyze the X-ray diffraction patterns and give information on the various phases present.

The significance of XRD as a characterization method as applied to nano-over layers is apparent. XRD requires between 1-3 weight percent of a particular phase to show up during a scan. A 5 nm over layer represents roughly $^{1}/_{1000}$ of a weight percent of the over all particle on a 5 μm nominal particle size. If the XRD pattern yields no conversion to nitride or carbide, that coupled with TEM micrographs confirming the over layer of the nitrides or carbides with subsequent atomic spacing and tripled with EDS for the nitrides showing a presence of nitrogen on the surface, but not in the interior of the particle is ample verification of the over layer formation.

C. Nitride Synthesis

Table 2: Performed reactions for Group VI nitride products.

Constituents	Sample	Description of Heating	Tube Size	Observations of Reaction
Chromium	JBB-1-2A	multiple 1 sec pulses	25 x 30 mm	
	JBB-1-2B	six 5 sec. pulses	25 x 30 mm	
	JBB-1-5B	5 min. sustained	25 x 30 mm	rxn. in 15 sec., blue streaks
	JBB-1-5C	3 min. sustained	25 x 30 mm	rxn. in 10 sec., blue streaks
	JBB-1-5D	1 min. sustained	25 x 30 mm	rxn. in 10 sec., blue streaks
Molybdenum	JBB-1-1A	3 min. sustained	25 x 30 mm	
	JBB-1-1B	2 min. sustained & ten 5 sec. Pulses	25 x 30 mm	
	JBB-1-1C	ten 10 sec. pulses	25 x 30 mm	
	JBB-1-8C	3 min. sustained	25 x 30 mm	rxn. in 10 sec., yellow-orange streaks
	JBB-1-8D	1 min. sustained	25 x 30 mm	rxn. in 8 sec., yellow-orange streaks
	JBB-1-8.2	1 hr. sustained	25 x 30 mm	rxn. in 15 sec., yellow-orange streaks

1. Chromium Nitride

a. Preparation and Firing

Chromium nitride represents the first of the Group VI nitrides studied. Group VI nitrides are important due to their high levels of catalytic activity in many of industry's key reactions. Again, since thin

over layers of nitrides have greater catalytic activity than the fully nitride product, in the following experiments an attempt to make thin over-layers was made.

Chromium Nitride (Cr_2N) has an adiabatic flame temperature of 1690 K. This is so when the ratio of Cr and N2 is 2:1 and the reactants are at 298 K and 1 atm pressure. This system lies in the zone near self-sustainability and this can be achieved through microwave ignition. Thus, self-sustainability of the reaction is to be avoided in order to obtain thin over layers.

The reaction was ignited using microwave energy. Chromium metal powder (1-5 micron in size) is used. The tube used is a 25 mm internal diameter tube and is filled with 5g of chromium metal powder. The nitrogen flow needed to fluidize the chromium powder was maintained and the tube vibrated with the help of the solenoid as explained in the experimental setup section.

In this system too, the instantaneous heating property of microwave energy is utilized to control the extent of the reaction. Therefore two types of reactions were performed as outlined in Table 1: one in which the microwave is kept on for longer periods (sustained reaction) and the other in which the microwave is intermittently turned on and off (pulsed reaction). The products from both reactions were analyzed using EDS, XRD and TEM.

b. Characterization Results

The XRD pattern of the chromium precursor powder and the product of experiment JBB-1-2B is shown in Figure 13 and 14 respectively. The XRD pattern for the product of experiment JBB-1-2B, the pulsed experiment, does not show any nitride peaks. It is important to remember that this is one of the assumptions necessary in the characterization of these over layers. When trying to characterize a nano-scaled over layer of nitride on a metal substrate, it is important to realize that the nitride represents less than one percent of the weight of the product. Under normal scan conditions, typically 3 weight percent is required of a particular phase to be identified using XRD. With no nitride phase present on XRD, one of the pieces to the puzzle is in place.

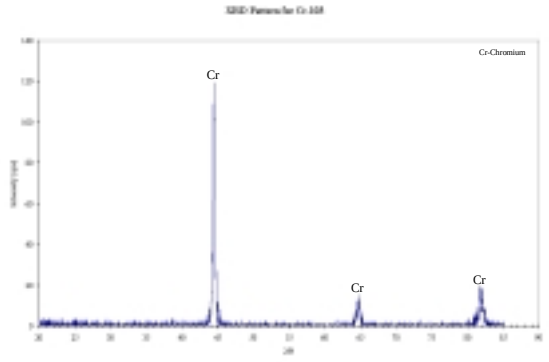

Figure 13: XRD pattern corresponding to chromium precursor powder used in the nitride experiments.

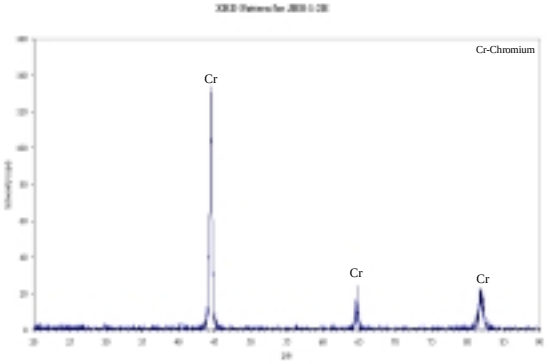

Figure 14: XRD pattern corresponding to JBB-1-2B.

The XRD pattern from the product of experiment JBB-1-5D, the five minute sustained microwave-heating shows Cr_2N peaks indicating conversion to nitride. A comparison with the XRD of chromium precursor powder shows that chromium peaks are also present for this sample. This indicates that conversion to nitride, as expected, is not complete.

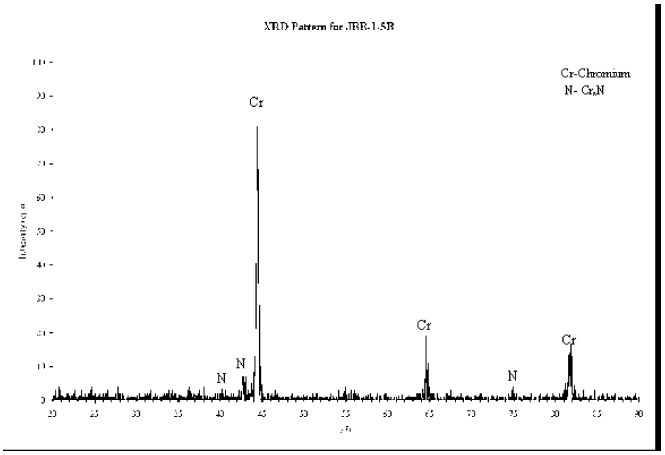

Figure 15: XRD pattern corresponding to JBB-1-5D.

EDS for the pulsed reaction (JBB-1-2B) was performed to verify the presence of surface nitrogen. The EDS graph at high kv located in Figure 16 does not show nitrogen, however at lower kV (Figure 17) there is presence of nitrogen. This sample did not show the presence of any nitride phase in the XRD, thus these low kv EDS images indicate that the nitrogen is present at the surface. Another piece of the puzzle is fit.

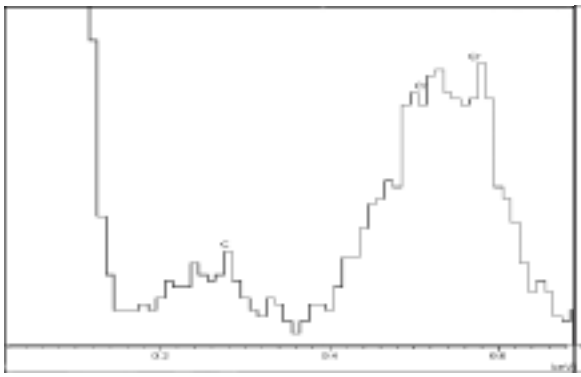

Figure 16: EDS pattern at 30 kV corresponding to JBB-1-2B.

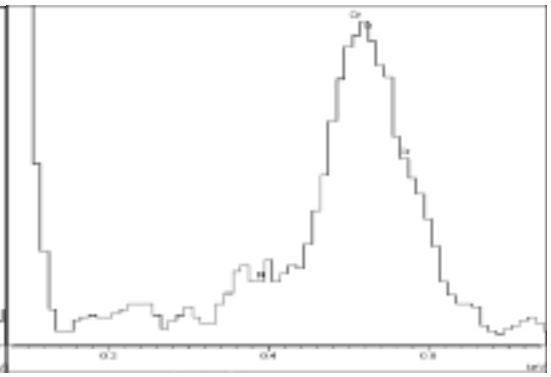

Figure 17: EDS pattern at 5 kV corresponding to JBB-1-2B.

TEM micrographs were obtained for both JBB-1-2B and JBB-1-5D. The red-white cane in Figure 18 represents the substrate corresponding to a d spacing of 2.04 A^o. The over layer is represented by the green-white cane and displays a d spacing of 2.24 A^o. With the scale in the upper left hand corner of the micrograph, the over layer is estimated to be 3-5 nm in width. These d spacings when compared with the literature values from JCPDS for those of chromium and Cr_2N correspond nearly perfectly. This comparison is shown in Table 3. This indicates the presence of a nitride phase in the over layer of the chromium substrate.

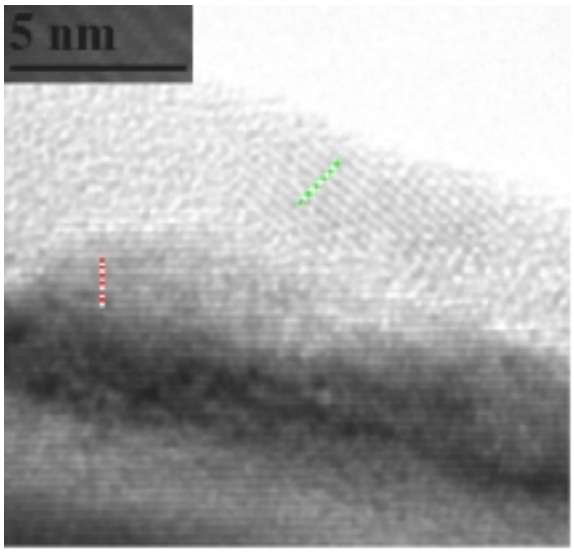

Figure 18: TEM micrograph of JBB-1-2B.

Table 3: d spacing values for Cr and Cr_2N for JBB-1-2B.

d-spacings for Cr, Cr2N (literature values)	
d spacings for Cr (A°)	**2.039**, 1.44, 1.17
d spacings for Cr_2N (A°)	**2.24**, 2.12, 1.64, 1.39, 1.269, 1.18

The red-white cane in Figure 14 represents the conversion to a bulk nitride phase corresponding to a d spacing of 1.64 A°. This d spacing is another verified value from JCPDS. This comparison is shown in Table 4. The conversion to nitride for this one-minute sustained heating reaction is clearly greater than that

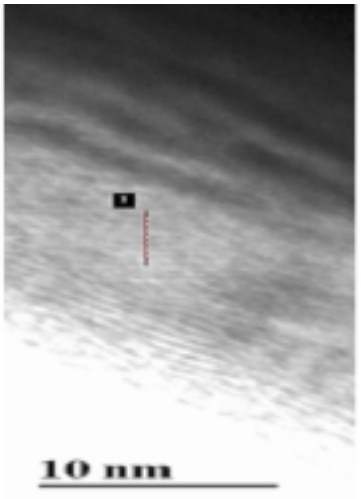

Figure 19: TEM micrograph of JBB-1-5D.

of the pulsed experiment. The reaction zone is substantially increased and penetrated farter into the substrate lattice. It is unclear from this image just how far the nitride does penetrate; however the fact that the nitride phase is present in the XRD pattern indicates substantial depth.

Table 4: Literature d spacing values for Cr and Cr_2N for JBB-1-5D.

d-spacings for Cr, Cr2N (literature values)	
d spacings for Cr (A^0)	2.039, 1.44, 1.17
d spacings for Cr_2N (A^0)	2.24, 2.12, 1.64, 1.39, 1.269, 1.18

c. Reaction Observations

Some observations during the JBB-1-5D reaction include the following. 1) Reaction was not observed immediately; the powders had to reach a certain temperature at which point reaction was observed. This occurred within ten seconds of turning on the microwave. 2) Once the reaction began, blue streaks were observed within the quartz tube, usually along the interior of the wall, with white sparking as well. This streaking appears to be arcing from the top steel sieve to the bottom steel sieve. 3) After one-minute time, the powder at the base of the tube began to glow red.

2. Molybdenum Nitride

a. Preparation and Firing

Efforts to obtain similar results for another group six nitride were made. The literature shows that the product is not stable above 1100 K. However there is a possibility of obtaining surface layers of nitride. The adiabatic flame temperature for this system using a Mo:N_2 ratio of 4:1 is 1095 K, which gives complete conversion. In the actual experiment, with the use of a fluidized bed, the nitrogen transport is not a limiting factor, rather the temperature becomes greater than 1100 K and thus decomposition of the nitride occurs. One key addition to this set-up involves the use of the high temperature ceramic paper for insulation to aid in the detainment of heat throughout the reaction.

Some experiments, similar to the ones for chromium nitride in identical conditions were performed. These are shown in Table 21. EDS, TEM and XRD were performed on the most promising product samples.

b. Characterization Results

XRD was performed on the molybdenum precursor powder and shown in Figure 20. XRD performed on JBB-1-8.2 shows no conversion to nitride in a one hour sustained microwave heating reaction. This is shown in Figure 21 indicating that no reaction took place or if the reaction had occurred only a thin layer was formed. As quantified in Table 2, other experiments were performed on this binary system. However, the fact XRD showed no phase change in the one hour sustained reaction it was not deemed necessary to characterize any of the other reactions. Once again, the fist piece of the puzzle is in place.

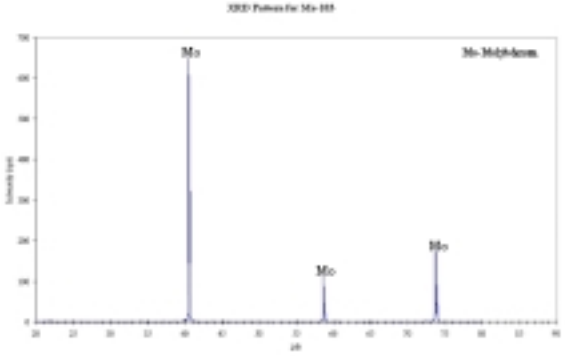

Figure 20: XRD pattern corresponding to molybdenum precursor powder used in nitride experiments.

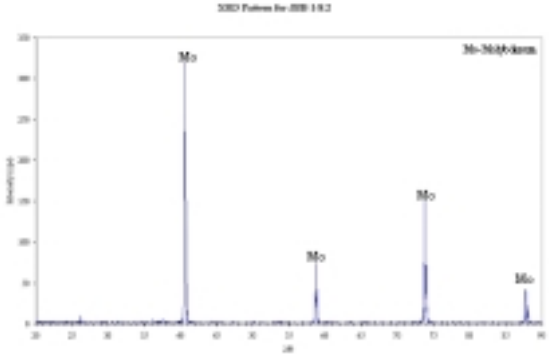

Figure 21: XRD pattern corresponding to JBB-1-8.2.

EDS at low kV was therefore performed on JBB-1-8.2 to verify the presence of surface nitrogen. A comparison of EDS at high kV (Figure 17) with EDS at low kV (Figure 18) for JBB-1-8.2 reveals the presence of this nitrogen only at the surface. The fact that XRD showed no presence of nitride adds another piece to the puzzle required to fully characterize the molybdenum nitride over layers.

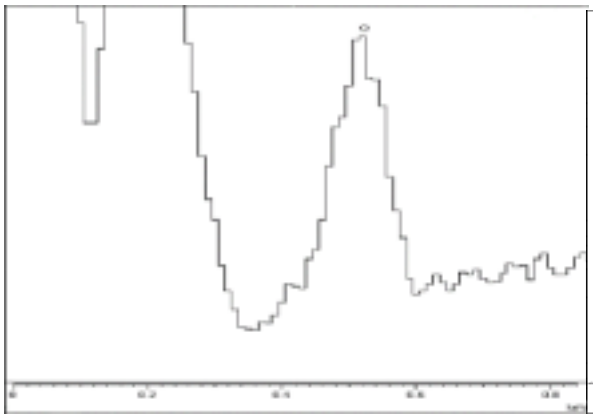

Figure 22: EDS pattern at 30 kV corresponding to JBB-1-8.2.

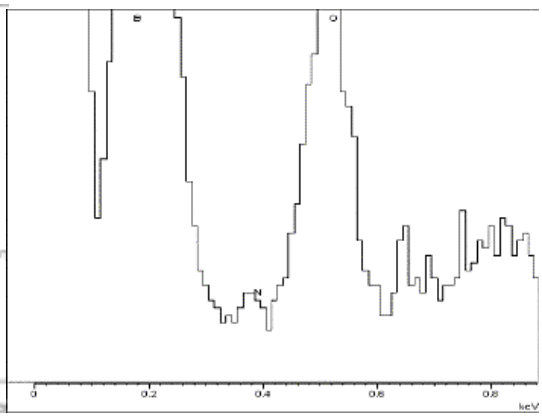

Figure 23: EDS pattern at 5 kV corresponding to JBB-1-8.2.

The TEM micrographs show interplanar spacing for this sample as 2.79 A^o. This spacing corresponds to the literature value of 2.80 A^o for MoN (Table 5). This indicates the presence of a nitride phase surrounding the molybdenum substrate when XRD results and EDS results are used in conjunction.

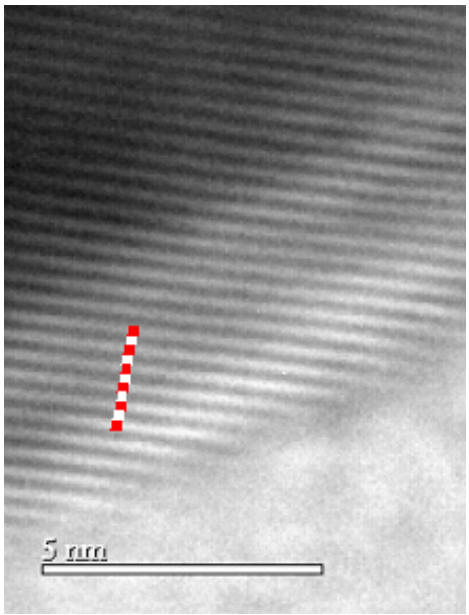

Figure 24: TEM micrograph of JBB-1-8.2.

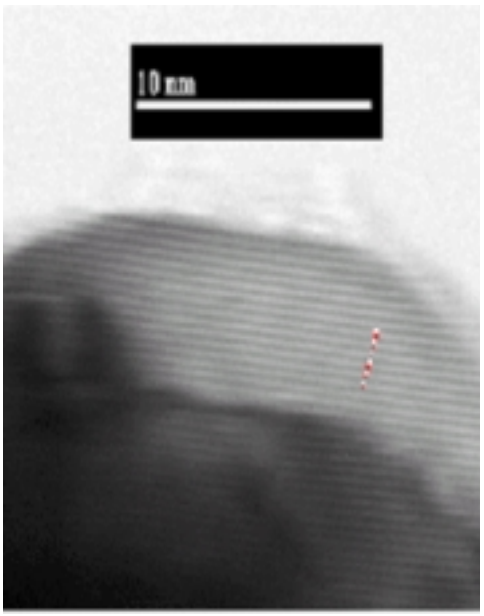

Figure 25: TEM micrograph of JBB-1-8.2.

Table 5: Literature d spacing values for Mo, MoN and Mo_2N for JBB-1-8.2.

d-spacings for Mo, MoN and Mo_2N (literature values)	
d spacings for Mo (A^o)	2.22, 1.57, 1.28
d spacings for MoN (A^o)	**2.80**, 2.48, 1.86,
d spacings for Mo_2N (A^o)	2.40, 2.08, 2.01, 1.47

c. Reaction Observations

Some observations during the JBB-1-8.2 reaction include the following. 1) Reaction was not observed immediately; the powders had to reach a certain temperature at which point reaction was observed. This occurred within eight seconds of turning on the microwave. 2) Once the reaction began, white sparking was observed, followed by yellow-orange streaks within the quartz tube. As the particles were fluidized in the N_2 gas flow away from the bed of particles in the lower portion of the tube, the appearance of what amounted to be shooting stars. The particle would begin to glow orange in color and then fizzle out as the particle returned to the stationary bed. 3) The powder at the base of the tube began to glow red.

D. Carbide Synthesis

Table 6: Performed reactions for Group VI carbide products.

Constituents	Sample	Description of Heating	Tube Size	Observations of Reaction
Chromium	JBB-1-11.1A	5 min sustained	13.5 x 19 mm	1) spark, 2) yellow fire-likeness, 3) blue bolts, 4) glowing red powder base
	JBB-1-11.1C	3 min. sustained	13.5 x 19 mm	1) spark, 2) yellow fire-likeness, 3) blue bolts, 4) glowing red powder base
	JBB-1-11E	fifteen 10 sec. pulses	25 x 30 mm	blue bolts were observed with yellow fire-like streaks within 40 seconds of ignition
	JBB-1-11F	ten 5 sec pulses	25 x 30 mm	
	JBB-1-11G	ten 3 sec. pulses	25 x 30 mm	
	JBB-1-11.2	1 hr. sustained	25 x 30 mm	
Molybdenum	JBB-1-3A	multiple 5 sec. pulses	25 x 30 mm	
	JBB-1-14E	ten 10 sec. pulses	25 x 30 mm	
	JBB-1-14C	3 min. sustained	25 x 30 mm	
	JBB-1-14D	1 min. sustained	25 x 30 mm	
	JBB-1-14.1A	5 min. sustained	13.5 x 19 mm	violent yellow sparking and flames
	JBB-1-14.1B	10 min sustained	13.5 x 19 mm	violent yellow sparking and flames
	JBB-1-14.2	1 min. sustained	25 x 30 mm	violent yellow sparking and flames, no bolts
Michal - Mody.	JBB-1-17.1B	5 min. sustained (not fluidized)	25 x 30 mm	yellow sparking and glowing red mixture base
	JBB-1-17.2	1 hr. sustained	25 x 30 mm	yellow sparking and glowing red mixture base

1. Chromium Carbide

a. Preparation and Firing

The synthesis of chromium carbide was performed using microwave-assisted ignition in a fluidized bed of argon gas. The adiabatic flame temperature for a Cr:C::3:2 reaction is 957 K. Microwave energy assists in the ignition of this reaction, which shows an adiabatic temperature well below the 1800 K required for self-sustainability.

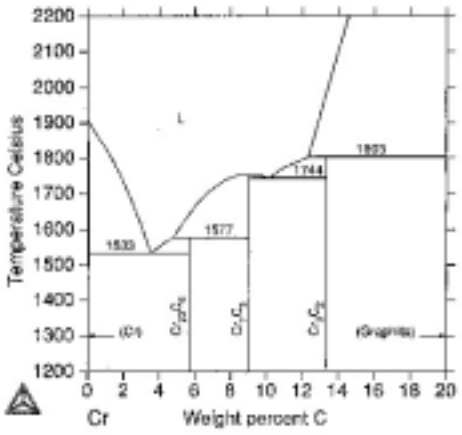

Figure 26: Phase diagram of the carbon-chromium system.

Chromium and black carbon powder 1-5 micron in size were used for the reaction. The powdered mixture of chromium and carbon was calculated to correspond to a stoichiometric ratio of 3:2. This is the equivalent of a 9 to 13 weight percent mixture of carbon to chromium as illustrated on the phase diagram in Figure 26. The reaction was carried out in a 25mm internal diameter quartz tube, which is filled with 5g of the mixture. The argon flow needed to fluidize the chromium and carbon powder mixture was maintained and the tube vibrated with the help of the solenoid as explained in the experimental setup section.

The firing of the products is divided in two main techniques, sustained and pulsed reactions. The sustained heating technique is performed in purpose and form to obtain a self-propagating product and therefore a bulk phase. The microwave oven was switched on and kept on for different periods. The time periods for the experiments were 3, 5 and 60 minutes. As with the nitrides, attempts to synthesize nano over layer formation were performed using different types of pulse times. The pulsed reactions, as outlined in Table 4, were carried out using a standard number of pulses, i.e. ten with varying times of 3,5 and 10 seconds. First however, the mixture was brought to reaction temperature through a sustained heating to the moment of observed reaction and then shut off. The argon flow needed to fluidize the chromium and carbon powder mixture was maintained and the tube vibrated with the help of the solenoid as explained in the experimental setup section.

The syntheses follow one of the two techniques: sustained or pulsed reaction. The first reactions performed were carried-out in the previously manufactured experimental set-up made of Teflon. Therefore, the attempts were unsuccessful in proper fluidization of the non-homogeneous reactant mixture. The required gas flow rate would cause the quartz tube to separate from the Teflon base. The reaction carried out in the improved experimental setup showed marked improvement. Since a low adiabatic flame temperature is characteristic of Cr_3C_2, a ceramic paper is wound around the tubes to reduce heat loss from the reaction system. TEM and XRD analysis were performed on the most promising product samples. EDS analysis would prove inconclusive in the case of the carbides due to the high percent of unreacted free carbon present in the product mixture.

b. Characterization Results

The XRD pattern for the chromium precursor powder is once again shown for comparison purposes in Figure 27. The XRD pattern of the two products that deemed worthy of characterization (i.e. JBB-1-11E and JBB-1-11.2) is shown in Figures 28 and 30 respectively. JBB-1-11E corresponds to a pulsed reaction consisting of fifteen 10-second pulses and JBB-1-11.2 represents a one-hour microwave heating reaction. A reaction performed by Akhil Jain in determining the feasibility of using a microwave environment to attempt to synthesize bulk Group VI transition metal carbides was also used in the comparison of heating methods. This method utilized no fluidization. The XRD pattern is shown for this reaction in Figure 29, below.

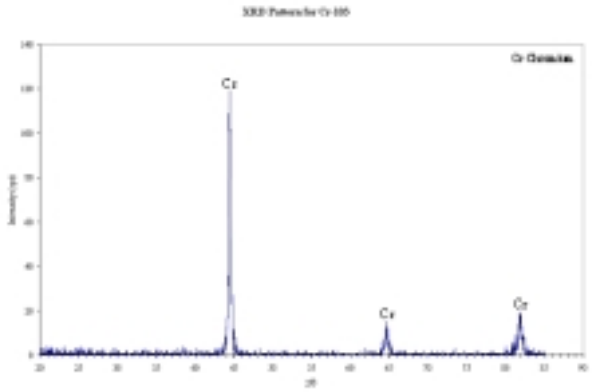

Figure 27: XRD pattern for Cr-103 precursor powder.

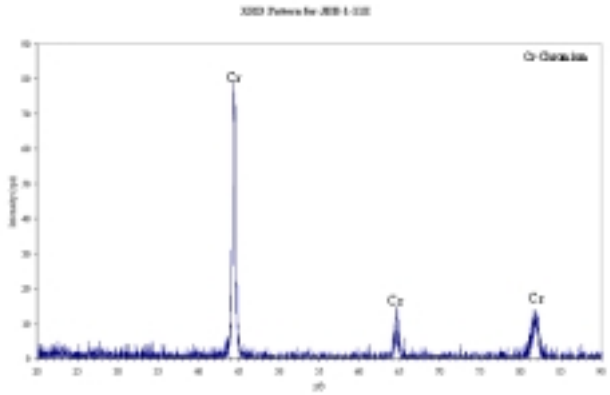

Figure 28: XRD pattern for JBB-1-11E.

The XRD for the product of the pulsed experiment (JBB-1-11E) does not show any carbide peaks. The results indicate no bulk transition to chromium carbide. This preliminary result can indicate a change just in the top surface of the powder sample.

The XRD pattern for the Akhil Jain ten minute unfluidized reaction is located in Figure 29. This clearly shows conversion to bulk carbide. The XRD pattern of JBB-1-11.2, the 1-hour sustained reaction, in Figure 30 shows increased conversion to bulk chromium carbide (Cr_2C_3). A comparison with the XRD of chromium precursor powder shows that chromium peaks are also present for this sample, indicating that conversion to carbide, as expected, is not complete. Note that the chromium peaks in the XRD are not broadened, indicating that some of the particles might not have reacted at all. It is worth noting that this particular scan would require a repeat do to the high background noise associated with it.

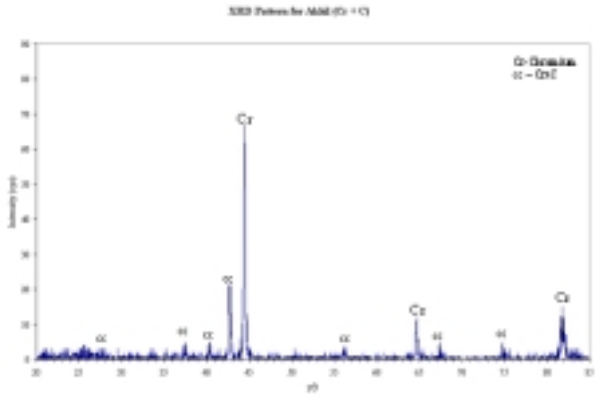

Figure 29: XRD pattern for Akhil Jain 10 minute unfluidized sustained reaction.

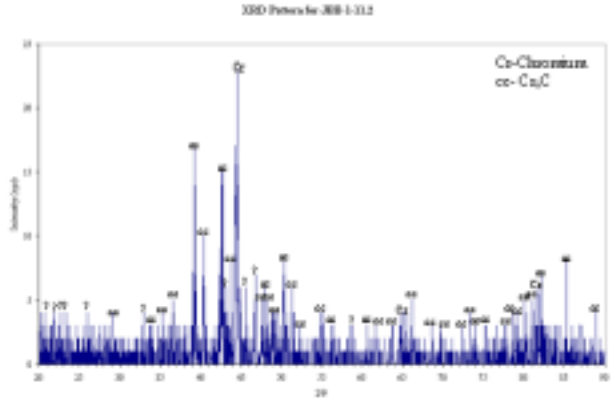

Figure 30: XRD pattern for JBB-1-11.2.

The TEM micrographs show interplanar spacing for JBB-1-11E as 2.75 A^o. This spacing corresponds to the literature value of 2.746 A^o for Cr_2C_3 (Table 7). This indicates the presence of a nitride phase surrounding the chromium substrate. From the TEM micrographs in Figures 31 and 32, respectively, it is plain to see that the over layer formation is not uniform in width nor is there uniformity in the coverage of the metal substrate. The answer to this observation lies in the question of how the carbon is transferred to the substrate during microwave heating in a fluidized bed of argon. It should be stated explicitly that there is a high transport limitation when manufacturing carbide over layers using this process. Amorphous carbon black is a very soft material when compared to that of chromium or molybdenum. As the particles are fluidized in a stream of argon and heated in the microwave, there are collisions between the carbon and the metal particles. As far as the author is concerned, there is no way to control the particle-to-particle interactions in this current set up. These collisions result in the transfer of carbon to the surface of the heated metal. From here, varying widths of carbide are formed corresponding to the amount of carbon deposited on the surface. Some particles show higher concentrations of carbide formed, while others show little or no phase change. Even further, some particles only indicate deposition of carbon resulting in an over layer of amorphous carbon only. This transport limitation is no present in the manufacture of nitride over layers because the second reactant is a gas and can react uniformly over the surface of the metal particle. Pulsing the microwave on and off results in over layer formation of chromium carbide, however uniformity of the over layer is sacrificed in the current set-up.

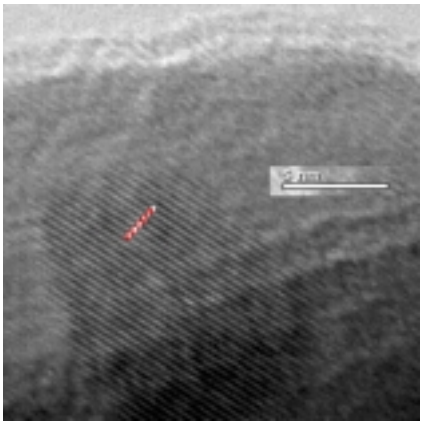

Figure 31: TEM micrograph of JBB-1-11E.

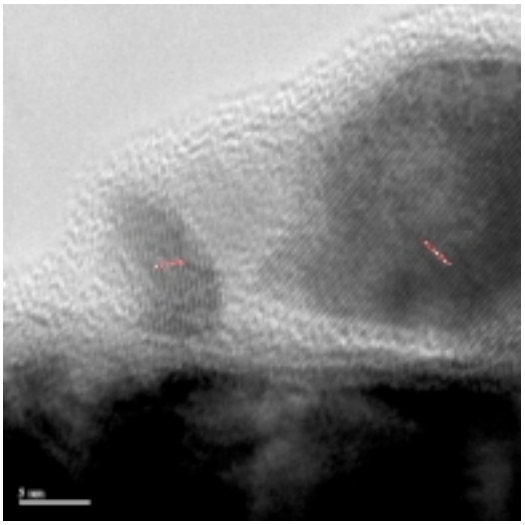

Figure 32: TEM micrograph of JBB-1-11E.

Table 7: Literature d spacing values for Cr, Cr_2C and Cr_3C_2 for JBB-1-11E and JBB-1-11.2.

d-spacings for Cr, Cr_2C and Cr_3C_2 (literature values)	
d spacings for Cr (A°)	2.04, 1.44, 1.17, 1.01, 0.912, …
d spacings for Cr_2C (A°)	2.11, 2.22, 1.63, 1.27, 1.17, …
d spacings for Cr_3C_2 (A°)	2.746, 2.547, 2.31, 2.25, 1.87, …

TEM micrographs were also taken of the one hour sustained reaction, i.e. JBB-1-11.2. This picture is shown in Figure 33. The most obvious difference in this micrograph image is the amount of conversion to chromium carbide in comparison to the pulsed reaction. There is no distinct layer formed, only bulk phase change as evident by the red and green canes showing identical d spacing at the surface and well into the particle. As explained above, the transport limitation is apparent when reacting two particles of differing species in the current set-up. In the case of JBB-1-11.2, the transport limitation is overcome and bulk phase change occurs. A medium, heating time needs be found somewhere in between short pulsing and long sustained heating where the optimal carbon transfer/carbide formation can occur.

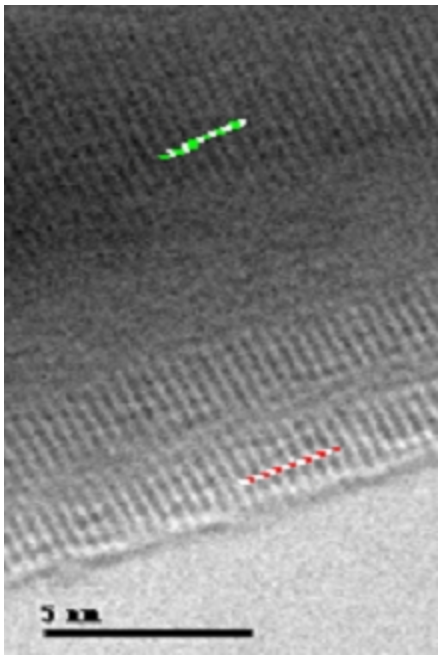

Figure 33: TEM micrograph of JBB-1-11.2.

c. Heat Treatment

A heat treatment process was explored to possibly remove the free unreacted carbon in the product mixtures. Also, it was thought that at the same time of removal of free unreacted carbon, the amorphous carbon over layers found on the metal substrates would also sublime away. If temperatures high enough to form chromium carbide could be achieved in an inert environment, the carbon over layers could be converted to uniform carbide over layers. This process involved a temperature of 800^{o}C, which literature has shown to be adequate for carbide formation. The temperature was increased 50^{o}C every 20 minutes until the high temperature of 800^{o}C was reached and held for 30 minutes.

Both JBB-1-11E and JBB-1-11.2 were heat treated in this manner and unfortunately the result of this treatment yielded a yellow product. This must be attributed to oxidation during the heat treatment. This is not what was expected to happen.

d. Reaction Observations

For a pulsed reaction, the mixture would be in a heating stage for roughly around 15-40 seconds. After this time reaction was observed. The microwave was shut off and the pulsing was begun. First, a white spark, followed by yellow fire-like streaks around the inside walls of the quartz tube were observed. Further more, blue lighting bolts, resembling arcing was observed from the top steel sieve to the bottom steel sieve. These were collimated in nature circumnavigating the interior of the quartz tube walls. Basically, a wall of bolts was observed. Sustaining the reaction for one hour resulted in very similar light pattern observations.

2. Molybdenum Carbide

a. Preparation and Firing

Molybdenum carbide, as indicated above, has shown very high levels of catalytic activity in the water-gas shift reaction. Also explained above, nano-scaled over layers of molybdenum carbide on the metal substrate would show increased catalytic activity over the bulk phase. The ultimate goal of this research was to synthesize molybdenum carbide, which has not been successful in the experimental set-up of Akhil Jain. In fact, no attempt to fluidize this reaction system was made.

The microwave-assisted ignition in a fluidized argon gas is used to perform the reaction. The adiabatic flame temperature for a Mo:C::2:1 reaction is 957 K. Microwave allows this reaction to ignite but not reach self-sustainability.

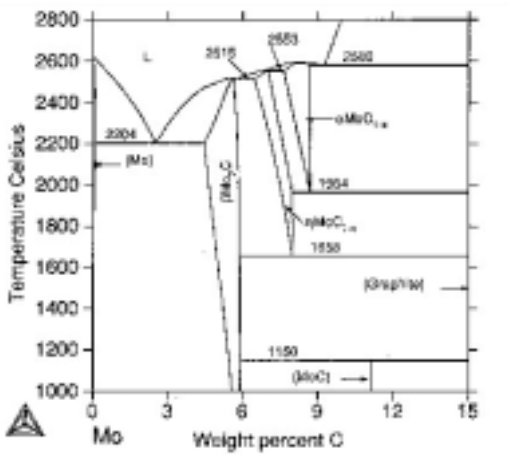

Figure 34: Phase diagram of the carbon-molybdenum system.

-325-mesh molybdenum powder that corresponds to 45 micron in size was used for the reaction. The carbon powder used was black carbon, 1-5 micron in size. The powdered mixture of molybdenum and carbon was prepared in a stoichiometric ratio of 2:1, corresponding to a 5.8 weight percent of carbon as indicated in the phase diagram corresponding to Figure 34. The reaction was carried out in a 25mm internal diameter quartz tube, which is filled with 5g of the mixture. The argon flow needed to fluidize the molybdenum and carbon powder mixture was maintained and the tube vibrated with the help of the solenoid as explained in the experimental setup section

The firing of the products is divided in two main techniques, sustained and pulsed reactions. The sustained heating technique is performed in purpose and form to obtain a self-propagating product and therefore a bulk phase. The microwave oven was switched on and kept on for different periods. The time periods for the experiments were 3, 5 and 60 minutes. As with the nitrides, attempts to synthesize nano over layer formation were performed using different types of pulse times. The pulsed reaction, as outlined in Table 4, was carried out with multiple five-second pulses. First however, the mixture was brought to reaction temperature through a sustained heating to the moment of observed reaction and then shut off. The argon flow needed to fluidize the chromium and carbon powder mixture was maintained and the tube vibrated with the help of the solenoid as explained in the experimental setup section.

The syntheses follow one of the two techniques: sustained or pulsed reaction. The first reactions performed were carried-out in the previously manufactured experimental set-up made of Teflon. Therefore, the attempts were unsuccessful in proper fluidization of the non-homogeneous reactant mixture. The required gas flow rate would cause the quartz tube to separate from the Teflon base. The reaction carried out in the improved experimental setup showed marked improvement. Since a low adiabatic flame temperature is characteristic of Mo_2C, a ceramic paper is wound around the tubes to reduce heat loss from the reaction system. TEM and XRD analysis were performed on the most promising product samples. EDS analysis would prove inconclusive in the case of the carbides due to the high percent of unreacted free carbon present in the product mixture.

b. Characterization Results

The XRD pattern for the molybdenum precursor powder is once again shown for comparison purposes in Figure 35. The XRD pattern of the two products that deemed worthy of characterization (i.e. JBB-1-14E and JBB-1-14.2) is shown in Figures 36 and 37 respectively. JBB-1-14E corresponds to a pulsed reaction consisting of ten 10-second pulses and JBB-1-14.2 represents a one-hour microwave heating reaction.

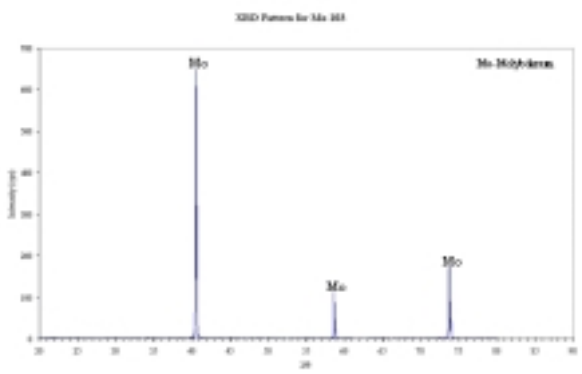

Figure 35: XRD pattern for Mo-102 precursor powder.

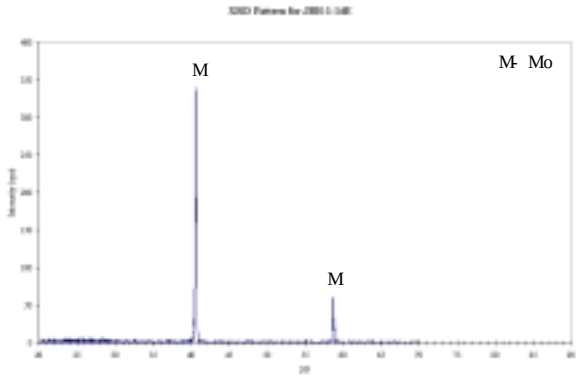

Figure 36: XRD pattern for JBB-1-14E.

The XRD for the product of the pulsed experiment (JBB-1-14E) does not show any carbide peaks. The results indicate no bulk transition to molybdenum carbide. This preliminary result can indicate a change just in the top surface of the powder sample.

The XRD pattern of JBB-1-14.2, the 1-hour sustained reaction, in Figure 37 shows no bulk phase change to molybdenum carbide. It is worth noting that similar results were observed for molybdenum

nitride as well. The pulsed reactions for that particular system not only did not yield any bulk transformation, but no over layer formation as well.

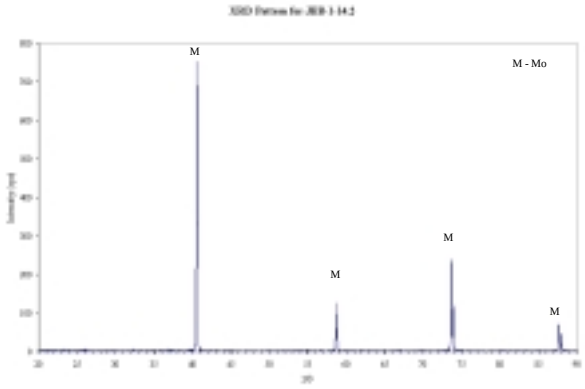

Figure 37: XRD pattern for JBB-1-14.2.

TEMs were obtained for these samples as well. The TEM from JBB-1-14E (pulsed reaction) in Figure 38 shows a deposit of amorphous carbon along the surface of the molybdenum substrate. As explained in the results section of this paper for chromium carbide, the carbon is transferred to the metal substrate through high temperature collisions during the reaction. The pulsed reaction, in this case, does not allow enough time or high enough temperature is not reached to successfully form over layers of molybdenum carbide.

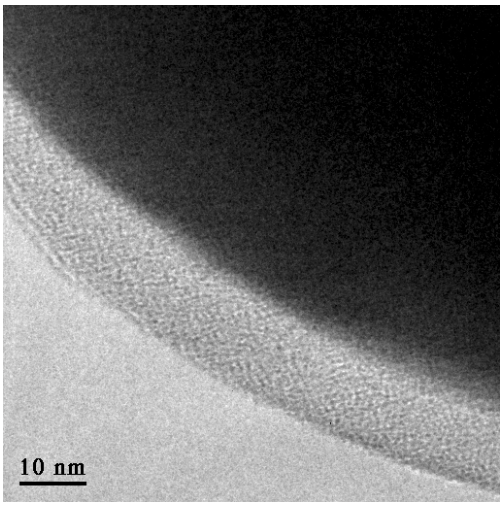

Figure 38: TEM micrograph of JBB-1-14E.

The TEM of the sustained reaction, JBB-1-14.2, shows d spacing for the sample to be 3.05 A^o as shown in Figure 39 and cross-referenced in Table 8. These spacing when compared with the literature values for those of Mo_2C shows the match between the Mo_2C peak. It definitely indicates a change in the top surface of the powder sample.

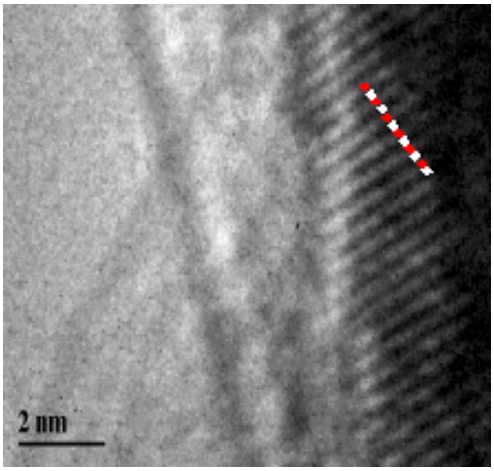

Figure 39: TEM micrograph of JBB-1-14.2.

Table 8: Literature d spacing values for Mo and Mo_2C for JBB-1-14E and JBB-1-14.2.

d-spacings for Mo and Mo_2C (literature values)	
d spacings for Mo (A^o)	2.22, 1.57, 1.28
d spacings for Mo_2C (A^o)	3.05, 2.61, 2.36, 2.28, …

c. Heat Treatment

A heat treatment process was explored to possibly remove the free unreacted carbon in the product mixtures. Also, it was thought that at the same time of removal of free unreacted carbon, the amorphous carbon over layers found on the metal substrates would also sublime away. If temperatures high enough to form molybdenum carbide could be achieved in an inert environment, the carbon over layers could be converted to uniform carbide over layers. This process involved a temperature of 800^{o}C, which literature has shown to be adequate for carbide formation. The temperature was increased 50^{o}C every 20 minutes until the high temperature of 800^{o}C was reached and held for 30 minutes.

Both JBB-1-14E and JBB-1-14.2 were heat treated in this manner. The results of this heat treatment were better than those observed for chromium carbide. Both Mo_2C products observed oxidation,

however, both samples also observed some conversion to molybdenum carbide. The XRD for both samples are shown in Figure 40 (pulsed reaction) and Figure41 (sustained reaction) respectively. The XRD for the pulsed sample shows oxidation peaks and what appears to be carbide peaks as well. The sustained sample shows a bulk conversion to oxide and molybdenum carbide as well.

A section of "Future Work" in this paper will outline further steps necessary in this realm.

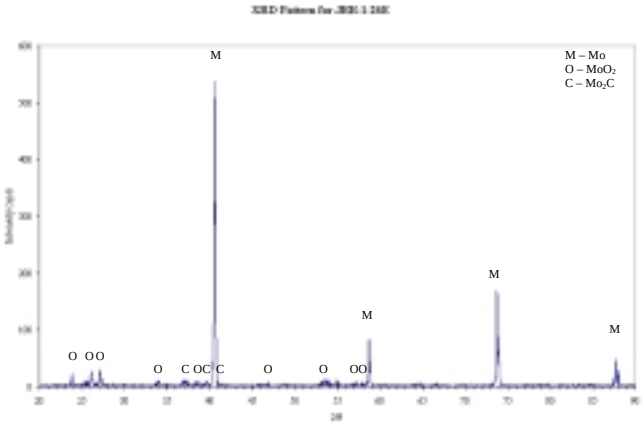

Figure 40: XRD pattern for post heat-treated JBB-1-14E.

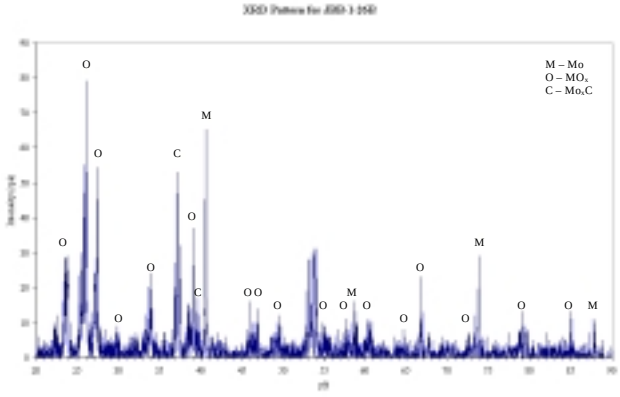

Figure 41: XRD pattern for post heat-treated JBB-1-14.2.

d. Reaction Observations

For a pulsed reaction, the mixture would be in a heating stage for roughly around 15-40 seconds. After this time reaction was observed. The microwave was shut off and the pulsing was begun. First, a white spark, followed by yellow fire-like streaks around the inside walls of the quartz tube were observed.

Further more, blue lighting bolts, resembling arcing was observed from the top steel sieve to the bottom steel sieve. These were collimated in nature circumnavigating the interior of the quartz tube walls. Basically, a wall of bolts was observed. Sustaining the reaction for one hour resulted in very similar light pattern observations.

3. Nickel-Molybdenum Carbide

a. Preparation and Firing

Previously performed research on transition metal carbides, following the scope of WGS, discovered bimetallic transition metal carbide high catalytic activity in the WGS.

The synthesis of Nickel-Molybdenum Carbide was performed using microwave-assisted ignition in a fluidized argon gas. The adiabatic flame temperature for Mo- Ni-C is uncertain because the reaction mechanism is unknown.

Molybdenum and black carbon powder size remain the same used for the molybdenum carbide synthesis. The nickel powder used was 45 micron in size. The powdered mixture of nickel, molybdenum and carbon is in a stoichiometric ratio of 1:1:1. The reaction was carried out in a 25mm internal diameter quartz tube, which is filled with 5g of the mixture. The argon flow needed to fluidize the nickel, molybdenum and carbon powder mixture was maintained and the tube vibrated with the help of the solenoid as explained in the experimental setup section. The firing of the combustion was performed using a sustained heating technique with two different periods of time: 5 and 60 minutes.

Post reaction observation of the product yielded an interesting find. There were two distinct products: a black powdered sample at the base of the tube and a light gray powder solid at the top of the tube attached to the mesh.

b. Characterization Results

The XRD of the two products in the quartz tube after reaction are shown in Figure 42 (product at bottom, JBB-1-17.2) and Figure 43 (product at top), respectively. The XRD for the product at bottom show peaks for Mo and peaks representing the formation of two other phases NiC, MoC. There is no

unreacted nickel present in this sample. The XRD of the product found in the mesh at the top shows Mo_2C peaks indicating conversion to carbide. As is apparent, the presence of unreacted molybdenum in this product is virtually non-existant, however, there was bulk phase change to molybdenum carbide. The mechanism is unknown at this time, but preliminary assumption tells the author that the nickel acted as either a heat trapper or a catalyst type addition to the reaction. The other peak ids are unreliable and need to be verified.

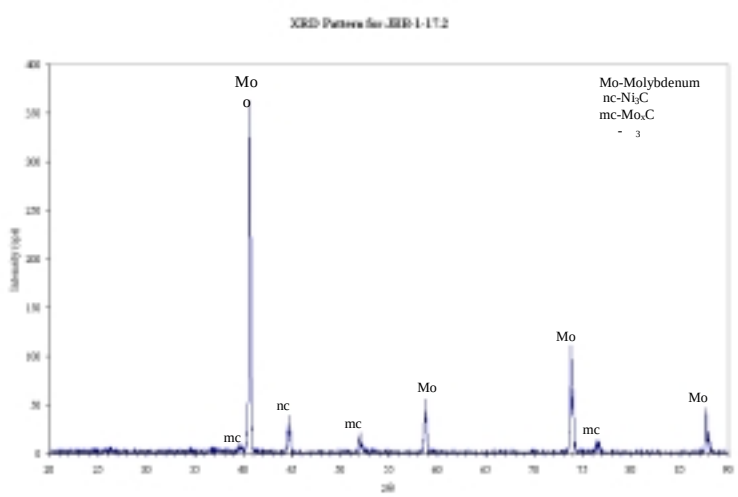

Figure 42: XRD pattern for JBB-1-17.2 (product at bottom).

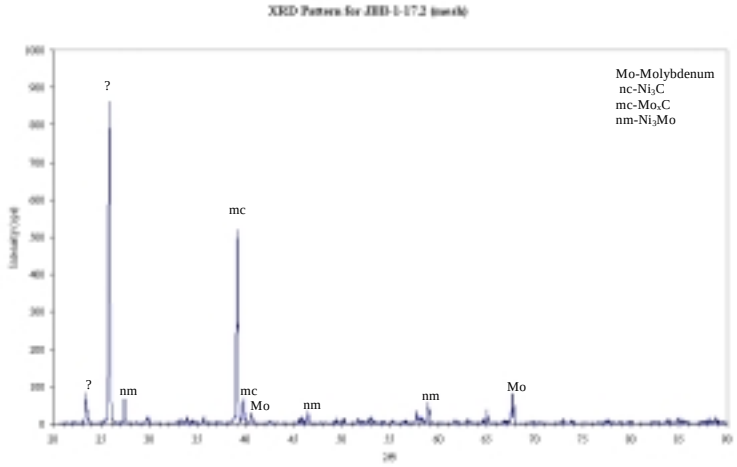

Figure 43: XRD pattern for JBB-1-17.2 (product at top).

IV. Summary

On a broad scale, the work of this 2002 NSF REU program illustrated and reiterated the success of utilizing self-propagating high temperature synthesis as a manufacturing technique to yield novel materials. Furthermore, utilizing microwave energy assistance in a vibrating fluidized bed the ability to control extent of reaction and product morphology was optimized.

More specifically, the production of nano-scale over layers of chromium and molybdenum metal nitrides and carbides was shown to be extremely successful. The fluidized bed eliminates the transport limitation inherent in traditional SHS for the production of the nitrides and carbides. Also, fluidization in an argon atmosphere of metal and carbon black particles has resulted in the production of carbides at the surface of the metal substrate.

Sustained and pulsed heating methods were explored for the varying systems resulting in different outcomes. Chromium nitride nano-scale over layers was produced with a heating method involving repeated short pulses of microwave energy, while bulk phase change occurred with a sustained microwave heating. Molybdenum fluidized in a nitrogen atmosphere, having a low adiabatic flame temperature, observed no phase change with pulsed heating. Over layers of molybdenum nitride were produced with a sustained heating method of one-hour. Chromium carbide nano-scale over layers was produced with a heating method involving repeated short pulses of microwave energy. The results indicate that amorphous carbon is deposited on the surface of the metal powder through particle collisions when fluidized in an inert gas atmosphere. Microwaves input enough energy to convert this surface carbon into chromium carbide. A sustained heating resulted in bulk phase. Molybdenum carbide observed no phase change with pulsed heating, but produced over layers with a sustained heating method of also one-hour.

All of the above nitride products were analyzed using SEM, EDS, XRD and TEM, while the carbide products were analyzed using SEM, XRD and TEM. To verify the formation of over layers, several items had to be in place: 1) no observed morphology change with SEM, 2) for the case of the nitrides, EDS had to give verification of surface nitrogen at low kV, but no presence of nitrogen at high kV, 3) XRD had to show no phase change and 4) TEM had to show d spacing at the surface corresponding to the desired ceramic.

In conclusion, the microwave assisted technique was shown to be successful in initiating metal, non-metal reactions with low adiabatic flame temperatures and also those reactions in which ignition of reaction was unsuccessful using the conventional tungsten filament (due to low adiabatic flame temperatures or excessive heat losses in the system). An attempt to reduce heat losses was made for various products by using various diameter quartz tubes for reaction, and also through the use of high temperature ceramic paper for insulation purposes. These results thus show that microwave assisted reaction is a promising technique of ignition for SHS reactions and can yield novel materials with thin over layers of ceramic materials over metal powder substrates that may have applications in catalysis or electronics.

V: Future Work

As indicated throughout the body of the paper, the investigation of microwave energy to propagate highly exothermic reactions to produce novel ceramic materials has been shown to be very successful. The method employed by Akhil Jain, as explained in his Masters of Chemical Engineering Thesis, was used with minor changes. To truly utilize this technology, however, several steps must be taken to further the work of Akhil and the author. These steps will be outlined in this section.

A. Microwave Technology

This section refers to the microwave-producing oven necessary in our setup. The current oven is primitive and does not address the necessary attributes that are needed to optimize this manufacturing method.

1. Variable Frequency Settings

The microwave employed during both the studies of Akil Jain and the author was a domestic microwave oven emitting a 245 GHz frequency. This frequency setting, utilizing the equation in the "Microwave Assisted Combustion Synthesis" section was calculated to be ideal for the goal of over layer formation. A microwave oven with the ability to vary the frequency setting to study such effects as percent conversion, bulk phase formation, depth of over layer formation and required time to drive systems with very low adiabatic flame temperatures. This could be accomplished by acquiring a microwave oven with the ability to vary the frequency setting.

2. Collimated Microwaves

The Amana domestic microwave currently used is calibrated for the heating of foods and beverages. This functionality results in a design mechanism where by the microwaves is reflected through out the interior of the oven thereby diffusing the microwaves into a non-concentrated beam. There exist microwave ovens that focus the microwaves not in a diffuse pattern, but in a concentrated beam directed precisely at the reaction zone. The microwave discharge would take place in a quartz cylinder around which a microwave resonant cavity fits. All of the energy created could then be utilized. The current

experimental apparatus or any subsequent improved experimental apparatus would benefit from this attribute.

3. Dual Microwave/Convection Oven

There are two methods to bring systems with low adiabatic flame temperatures to the point of reaction. Those two methods are constant input of energy and raising the pre-reaction temperature of the reactants to a point where local ignition will produce self-sustainability. In the current experimental set-up, it is very difficult to preheat the powders to this level and then make the transfer to the microwave oven for reaction. A hybrid convection/microwave heating apparatus that allows this pre-reaction heating would be of great benefit to this project.

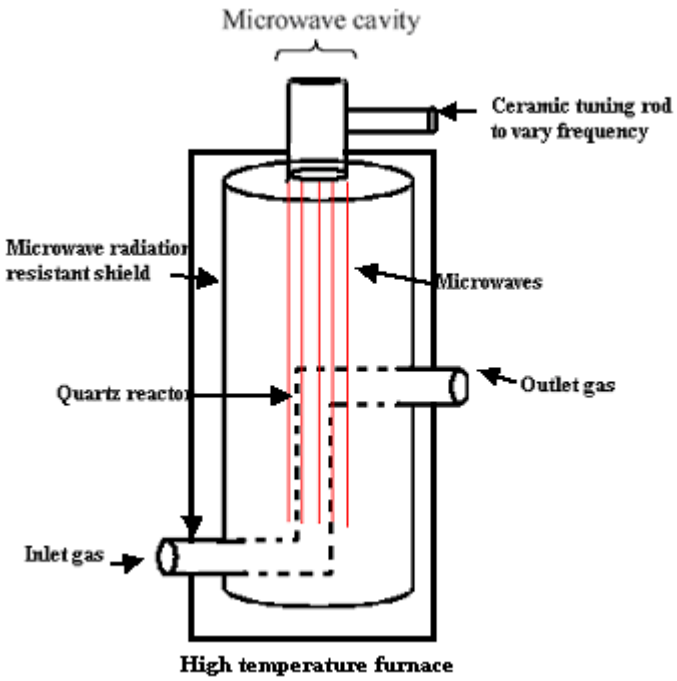

Figure 44: Preliminary design of heating device.

B. Experimental Apparatus and Fluidization Method

This section refers to the current non-optimized experimental set-up and fluidization method. While the current apparatus has addressed some of the issues including airtight seals and keeping the quartz tube reactor in place during reaction, other issues have become obvious that need to be dealt with. These

items include the use of the stainless steel sieve to keep the metal powders within the reaction tube, the weight of the current apparatus, etc.

1. High-Speed Camera Work

During reaction, there are several key attributes that have been observed. These include self-sustaining waves in the case of chromium carbide, glowing beds of particles for all systems, fire-like flames for all systems, violent sparking for all systems and what appears to be arcing from one steel sieve to the other steel sieve for all systems. All of these intriguing observations warrant a closer look. The only accurate way to approach this is with a high-speed shutter camera. With this addition, frame after frame in real time could be captured and studied. The reaction with the nitrogen gas in the case of the nitrides could be studied and quantified. Also, the deposition of carbon on the metal substrates and subsequent conversion to carbide could be observed. Not to mention the ability to accurately look at the arcing mechanism observed in the current set up.

With the revised heating apparatus, it would have to be designed with the ability to be transparent for the camera set up to be used properly.

2. Plasma State of Matter

Along with the observation of arcing between the steel sieves, microwaves generate energy that ionize and heat the gas into plasma upon ignition with the metal particles. The cavity may be tuned with a ceramic tuning rod to optimize the frequency. Theoretically, the plasma contains metastable N_2 as well as N^+, N^{2+} and free electrons. Further study of this interesting result of microwave heating is warranted and could result in a better manufacture angle to approach.

3. Fluidization Without Stainless Steel Sieve

Large-scale industrial processes utilize a method of fluidization that requires no mechanism by which the solid reactants are held within the reaction zone. The fluidizing gas is brought to the reactants through what amounts to be a 90^o turn. When the fluidizing gas is turned off the solid reactants pack down, while when the gas is turned on the bed of particles expands with no blockage required. A similar idea must

be employed here. During reaction in the current set-up, the sieve becomes clogged thereby reducing the flow of the fluidizing gas that increases the transport limitation and ultimately reduces the effectiveness of this set-up.

4. Calculations Required to Accurately Measure Fluidizing Gas Flow Rate

As explained in the ***"Combustion Synthesis in a Fluidized Bed"*** section of this report there exists an optimum gas flow rate that results in the proper fluidization of all of the systems discussed. Calculations need to be done to quantify what exactly these flow rates are and in turn need to be reproduced for every experiment run. This flow rate needs to be high enough to successfully fluidize the particles, but low enough to not allow the particles to escape in the outlet gas stream. Also once this benchmark is set, experiments by which the flow rate is fluctuated could be performed to observe the effects of the flow rate on the conversion.

C. Precursor Particle Size

With the current setup, a limitation exists in the direction the experiments can go in terms of varying the precursor particle size. This direction involves the development of a catalyst support system or the manufacture of high surface area porous metal substrates. The avenue that cannot be explored in the current setup is decreasing the particle metal substrates to the nano-scale. The author feels very small particles with very thin over layers would be the best alternative to explore. In terms of catalytic applications, the current products do not have the required surface area necessary to compete with industry standard catalysts.

D. Improved Heat Treatment Process

As discussed in the experimental portion of this paper, a crude high temperature heat treatment was performed to attempt to burn off the thick layer of amorphous carbon at the surface of the metal substrate and convert the amorphous carbon directly at the interface zone to carbide compounds. Also, the free unreacted carbon in the product mixture would hopefully vaporize. Preliminary results in an argon atmosphere at 800^{o}C yielded an undesirable outcome as explained in the various carbide results sections of

this paper. Further journal exploration is required to develop a useable heat treatment method to perform the above task.

E. Bimetallic Substrates

Recent research in the area of Group VI nitrides and carbides has clearly shown high catalytic activity levels. With the addition of a second transition metal such as cobalt and nickel, these compounds exhibit even higher activity levels over their one metal counterpart. An example of this is shown in Figure _, where the bimetallic carbides show higher levels of catalytic activity than molybdenum carbide. The possibility of starting with bimetallic substrates, basically alloys or solid solutions of these elements, and attempting to place carbide over layers with this manufacture method should be explored.

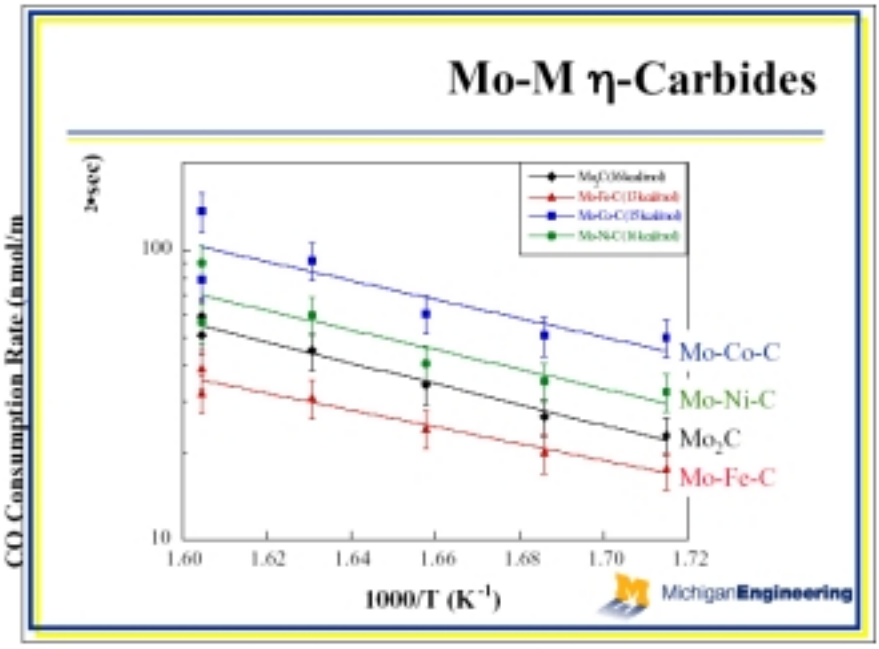

Figure 44: Bimetallic carbides and corresponding activity levels for the water gas shift reaction [20].

F. Catalytic Testing

Transition metal nitrides and carbides, especially with nano-scale features have been shown to be potential replacements for traditional hydrodenitrogenation (HDN) and hydrodesulphurization (HDS) catalysts [11-13]. To be able to verify the novelty of these materials and also to ascertain that the thin films

formed are of catalytic value the materials formed should be tested for catalytic activity in hydrodesulphurization reactions and hydrodenitrogenation reactions. The prime candidate materials for such an investigation on the basis of this work would be chromium nitride and molybdenum nitride. Chromium nitride and molybdenum nitride being group six metal nitrides would be of most value since these group six materials have been shown to have highest catalytic activity.

Furthermore, the carbides produced must be tested for catalytic activity in the water-gas shift reaction in proton exchange membrane fuel cells.

The catalysis lab in the University of Illinois's Chemical Engineering Department operated by Professor J. R. Regalbuto performs these techniques routinely.

G. Further Characterization

To better estimate the thickness of the thin layers formed, Secondary Ion Mass Spectroscopy could be performed on the samples. However, this measurement would be difficult considering the powders used are very small. X-ray Photoelectron Spectroscopy could also be performed on the samples, which would give the oxidation state of the elements present on the thin over layers. This would be helpful in determining the phase of the over layer formed.

References

[1] Thompson, L. T., "DOE CARAT – University of Michigan Phase 2 Results," http://www.ipd.anl.gov/carat/1998projects/umich_results2.htm, July 9, 2002.

[2] A. Varma, A.S. Rogachev, A. S. Mukasyan, "Combustion Synthesis of Advanced Materials: Principles and Applications," *Adv. in Ch. Eng.*, **24**, 79-226 (1998).

[3] A. Varma, "Form From Fire," *Scientific American*, **45**, 58-61 (2000).

[4] Z.A. Munir, "Synthesis of High Temperature Materials by Self-Propagating Combustion Methods." *Am. Ceram. Soc. Bull.*, **67,** 342-49 (1988).

[5] Z.A. Munir, U. Anselmi-Tamburini, "Self-Propagating Exothermic Reactions: The Synthesis of High-Temperature Materials by Combustion," *Mater.Sci.Reports***,** **3**, 277-365 (1998).

[6] A. Varma, J. P. Lebrat, "Combustion Synthesis of Advanced Materials," *Chem. Eng. Sci.*, **47**, 2179 (1992).

[7] Moore John J., Feng H. J., "Combustion Synthesis of Advanced Materials: Part I Reaction Parameters," *Progress in Materials Science*, **39**, 243-273 (1995).

[8] Sutton W. H., "Microwave Processing of Ceramic Materials," *Ceramic Bulletin*, **68** (2), 376-386 (1989).

[9] Roy R., Agrawal D., Cheng J., Gedevanishvili S., "Full Sintering of powdered-metal bodies in a microwave field," *Nature***,** **399**, 668-670 (1999).

[10] Cheraddi A., Desgardin G., Provost J., Raveau B., "Electric magnetic field Contributions to the microwave sintering of Ceramics," *Electroceramics IV*, **II**, 1219-1224 (1994).

[11] Oyama S. T., "Preparation and Catalytic Properties of Transition Metal Carbides and Nitrides," *Catalysis Today*, **15**, 179-200 (1992).

[12] Chen J. G., "Carbide and Nitride Overlayers on Early Transition Metal Surfaces: Preparation, Characterization and Reactivities," *Chem. Rev.*, **96**, 1477-1499 (1996).

[13] Colling C. W. and Thompson, L. T., "The Structure and Function of Supported Molybdenum Nitride Hydrodenitrogenation Catalysts," *Journal of Catalysis*, **146**, (1), 193-203 (1994).

[14] Choi J. G., Brenner J. R., Colling C. W., Demczyk B. G., Dunning J. L., Thompson L. T., "Synthesis and Characterization of Molybdenum nitride Hydrodenitrogenation catalysts," *Catalysis Today*, **15**, (2), 201-222 (1992).

[15] Choi J. G., Curl R. L., Thompson L. T., "Molybdenum nitride catalysts: 1. Influence of the synthesis factors on structural properties," *Journal of Catalysis*, **146**, (1), 218-227 (1994).

[16] Dolce G. M., Savage P. E., Thompson L. T., "Hydro-treatment activities of supported molybdenum nitrides and carbides," *Energy and Fuels*, **11** (3), 668-675 (1997).

[17] Hyeon T., Suslick K. S., Li S, Lee J. S., "Catalytic hydrogenation of Indole over molybdenum nitride and carbides with different structures," *Applied Catalysis*, **A: General 184**, 1-9 (1999).

[18] Schalatter J., Oyama S., Metcalfe, J.E. and Lambert, J. M., *Industrial Eng. Chem.* **Res 27**, 1648 (1988).

[19] Patt. J. Moon, Phillips D. J., Thomson, L., *Catalysis Letters* in press 1999.

[20] Thompson, L. T., "Novel Water Gas Shift Catalysts," http://www.eren.doe.gov/hydrogen/pdfs/nn0123aw.pdf, July 1, 2002.